Article

Structure-Based Design of an Iminoheterocyclic beta-Site Amyloid Precursor Protein Cleaving Enzyme (BACE) Inhibitor that Lowers Central A# in non-Human Primates

Mihirbaran Mandal, Yusheng Wu, Jeffrey Misiaszek, Guoqing Li, Alexei V. Buevich, John P. Caldwell, Xiaoxiang Liu, Robert D. Mazzola, Peter Orth, Corey Strickland, Johannes H. Voigt, Hongwu Wang, Zhaoning Zhu, Xia Chen, Michael Grzelak, Lynn A. Hyde, Reshma Kuvelkar, Presscott T. Leach, Giuseppe Terracina, Lili Zhang, Qi Zhang, Maria S. Michener, Brad Smith, Kathleen Cox, Diane Grotz, Leonard Favreau, Kaushik Mitra, Irina Kazakevich, Brian A. McKittrick, William J Greenlee, Matthew E. Kennedy, Eric M. Parker, Jared N Cumming, and Andrew W Stamford

J. Med. Chem., **Just Accepted Manuscript** • DOI: 10.1021/acs.jmedchem.5b01995 • Publication Date (Web): 03 Mar 2016

Structure-Based Design of an Iminoheterocyclic beta-Site Amyloid Precursor Protein Cleaving Enzyme (BACE) Inhibitor that Lowers Central Aβ in non-Human Primates

Mihirbaran Mandal,[‡],Yusheng Wu,[‡] Jeffrey Misiaszek,[‡] Guoqing Li,[‡] Alexei Buevich,[‡] John P. Caldwell,[‡] Xiaoxiang Liu,[‡] Robert D. Mazzola,[‡] Peter Orth,[‡] Corey Strickland,[‡] Johannes Voigt,[‡] Hongwu Wang,[‡] Zhaoning Zhu,[‡] Xia Chen,[§] Michael Grzelak,[§] Lynn A. Hyde,[§] Reshma Kuvelkar,[§] Prescott T. Leach,[§] Giuseppe Terracina,[§] Lili Zhang,[§] Qi Zhang,[§] Maria S. Michener,[∥] Brad Smith,[∥] Kathleen Cox,[#] Diane Grotz,[#] Leonard Favreau,[#] Kaushik Mitra,[#] Irina Kazakevich,[⊥] Brian A. McKittrick,[‡] William Greenlee,[‡] Matthew E. Kennedy,[§] Eric M. Parker,[§] Jared N. Cumming,[*,‡] and Andrew W. Stamford[*,‡]

[‡]Department of Global Chemistry, [§]Department of Neuroscience, [∥]Department of Safety Assessment and Laboratory Animal Research, [⊥]Department of Discovery Pharmaceutical Sciences, and [#]Department of Pharmacokinetics, Pharmacodynamics, and Drug Metabolism

Merck Research Laboratories, 2015 Galloping Hill Road, Kenilworth, NJ 07033.

Abstract:

We describe successful efforts to optimize the in vivo profile and address off-target liabilities of a series of BACE1 inhibitors represented by **6** that embodies the recently-validated fused pyrrolidine iminopyrimidinone scaffold. Employing structure-based design, truncation of the cyanophenyl group of **6** that binds in the S3 pocket of BACE1 followed by modification of the thienyl group in S1 was pursued. Optimization of the pyrimidine substituent that binds in the S2'-S2" pocket of BACE1 remediated time-dependent CYP3A4 inhibition of earlier analogs in this series and imparted high BACE1 affinity. These efforts resulted in the discovery of difluorophenyl analogue **9** (MBi-4) which robustly lowered CSF and cortex Aβ_{40} in both rats and cynomolgus monkeys following a single oral

dose. Compound **9** represents a unique molecular shape among BACE inhibitors reported to potently lower central Aβ in non-rodent preclinical species.

Introduction

Alzheimer's disease (AD), is a progressive neurodegenerative disorder that affects an estimated 5.3 million people in the United States and is responsible for 60 – 80% of all dementias, of which there were nearly 47 million worldwide in 2015.[1,2] In addition to the emotional and social burden that AD exerts on patients and their families, the economic burden is enormous. In the US alone, the total cost of care for patients with AD and other dementias was approximately US $226 billion in 2015.[1] It is expected that the number of people with AD will triple by 2050 resulting in a public health crisis unless disease modifying agents become available.[1,2] Since current AD medications, the acetylcholine esterase inhibitors and the *N*-methyl-D-aspartate receptor antagonist, memantine, only produce modest and transient improvements in cognitive function,[3] there is an urgent medical need to discover an agent that slows the underlying neurodegenerative process. Major advances in the fields of genetics, cell biology, biochemistry and neuroscience have provided some level of understanding of the pathophysiology of AD.[4] Two major neuropathological hallmarks of AD are extracellular amyloid plaques and intracellular neurofibrillary tangles which are found predominantly in the cortex and hippocampus. Amyloid plaques are composed of oligomerized and fibrillar *β*-amyloid (A*β*) peptides, primarily 42 amino acid residues in length, which are derived from amyloid precursor protein (APP) through sequential cleavage of APP by the beta-site APP cleaving enzyme 1 (BACE1) followed by γ-secretase.[5] According to the amyloid hypothesis, accumulation of A*β* peptides in the brain is causative of the underlying neurodegenerative process of AD. Therefore, inhibition of A*β* peptide synthesis is a potentially disease-modifying approach to the treatment of AD.

Over recent years, BACE1 inhibition has emerged as the primary small molecule approach for blocking Aβ peptide synthesis given the mechanism-based toxicity that attends γ-secretase inhibition, resulting in dose-limiting side effects.[6] Complementary approaches targeting central Aβ via anti-Aβ monoclonal antibodies have also been tested in the clinic, but the effects on cognitive improvement reported thus far either did not meet their target endpoints or, if they were significant, represented only a minimal effect and require further trials.[7] Taken together, the clinical data generated to-date with both γ-secretase inhibitors and anti-Aβ antibodies do not reflect a definitive or even robust vetting of the amyloid hypothesis.

In support of a focus on BACE1 inhibition to ultimately test this hypothesis, BACE1 knockout (KO) mice do not produce Aβ peptides,[8] and a cross between these knockout mice and a transgenic mouse model of early onset Alzheimer's disease showed significant improvement in the overall disease phenotype in regard to both reduction of amyloid levels and decreased memory deficits.[9] BACE1 KO mice were initially reported to possess no overt negative phenotype,[8] but more recently loss of BACE1 function in these animals has been shown to result in subtle morphological and behavioral alterations, and physiological non-APP substrates of BACE1 have been identified.[10] Among the best characterized of these substrates is neuregulin 1, both type III and type I. Phenotypes associated with reduced proteolytic processing of these two substrates in BACE1 KO mice are a reduction of peripheral nerve myelination[11] and a reduction in muscle spindle formation,[12] respectively. Importantly, these and many phenotypes in homozygous BACE1 KO mice are not seen in BACE1 heterozygous mice and are not replicated in adult wild type mice given selective BACE inhibitors. While our understanding of BACE1 biology continues to evolve, and careful monitoring of safety in BACE1 inhibitor clinical trials is critical, the sum total of current data offers the potential for partial pharmacological inhibition of BACE1 in adult patients to be a safe approach to disease modification in Alzheimer's disease.

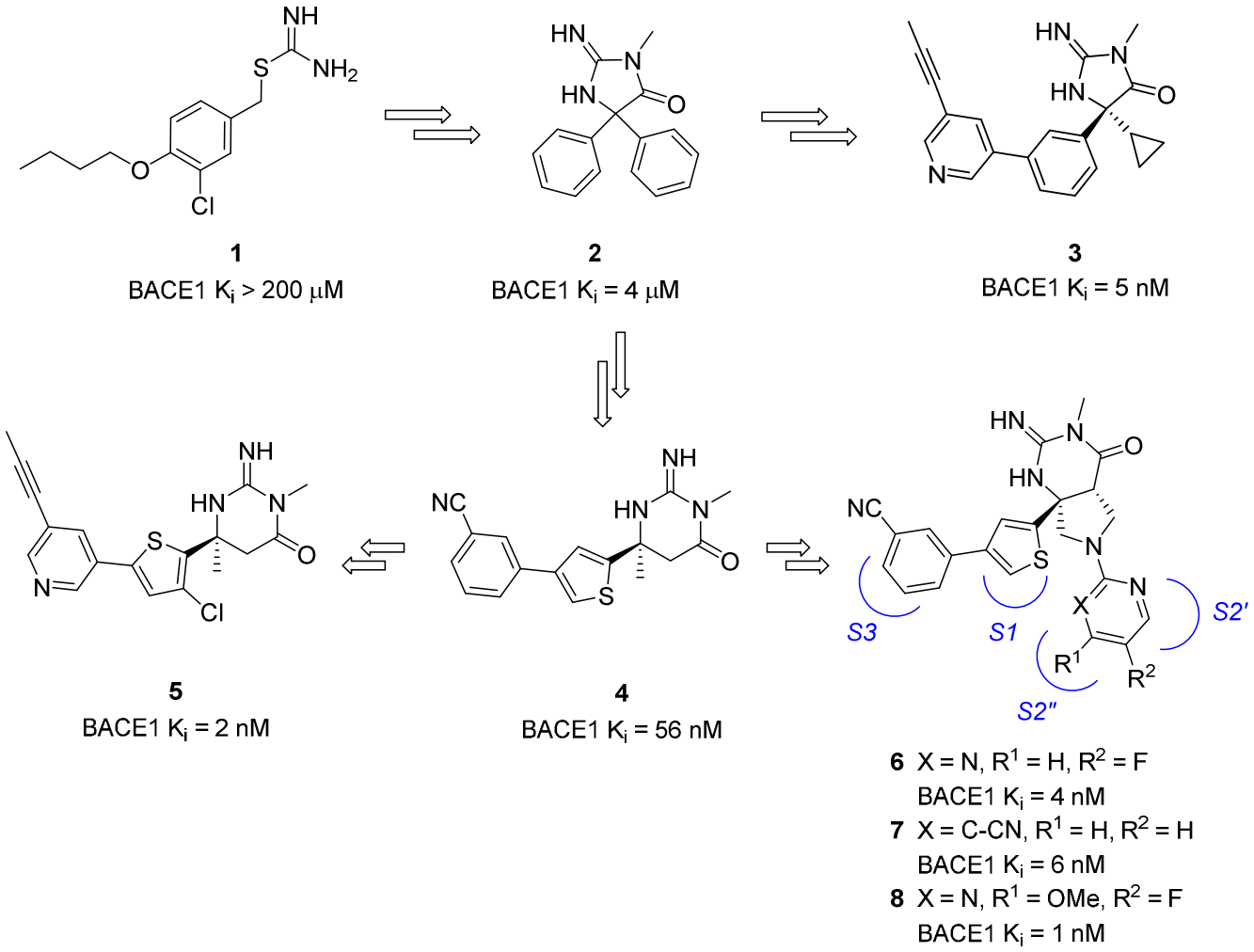

Figure 1: Discovery of bicyclic iminopyrimidinones **6**, **7** and **8** from fragment **1** by rational design and SAR development through iminohydantoins **2** and **3** and iminopyrimidinone **4**.

Because BACE1 is an aspartyl protease, the early phase of BACE1 inhibitor design was dominated by substrate-based peptidic and peptidomimetic approaches[13] that had been successful in the design of inhibitors of related aspartyl proteases, such as HIV protease and renin. These efforts resulted in many potent inhibitors, but these generally lacked suitable molecular properties to achieve significant brain penetration and *in vivo* CNS Aβ lowering activity at appropriate pharmacological doses.[14] Therefore, focus shifted to non-peptidic BACE1 inhibitors that would be more likely to possess properties conducive to CNS activity.

As shown in Figure 1, our work in this area began with the identification of isothiourea **1** through a fragment based approach,[15] and we have disclosed the progression of this fragment via lead compound **2**[16] to high affinity brain penetrant and bioavailable inhibitors belonging to two distinct chemical series, iminohydantoins (*e.g.* **3**)[17] and iminopyrimidinones (*e.g.* **4** and **5**).[18] These efforts,[19] independent of others achieved through HTS and fragment based approaches,[20] involved significant de novo design elements with extensive application of X-ray crystallography and molecular modeling. In the iminopyrimidinone series, additional SAR development that focused on structural diversity and conformational constraint led to design of a novel bicyclic iminopyrimidinone scaffold represented by compounds **6**-**7**[21] and **8** (Figure 1).

Compound **6** reduced cortex Aβ_{40} in Sprague Dawley rats (-42% compared to vehicle) after administration of a single dose (30 mg/kg, PO).[21] Unfortunately, it had relatively high PSA that likely contributed to modest brain penetration (brain/plasma 0.1), was a potent time dependent CYP3A4 inhibitor and showed significant *h*ERG inhibition (70% @ 1 μM). To overcome these issues, we investigated truncation of the cyanophenyl moiety of **6** that binds in the BACE1 S3 pocket (shown schematically in Figure 1). We concurrently explored SAR of the fluoropyrimidine group of **6** that binds in the S2'-S2" pockets to rescue the associated loss of affinity and to address the time-dependent CYP3A4 inhibition. Subsequent modification of the aryl group in S1 was pursued to further improve the affinity and selectivity of the series. These efforts culminated in discovery of inhibitor **9** (MBi-4; Figure 2) which showed robust pharmacodynamic Aβ lowering activity in rats and monkeys. It is worth noting that the vast majority of published small molecule BACE inhibitors that lower Aβ in monkey and / or dog, including all that have entered clinical trials, have substituents that occupy the S3 subsite of BACE, and none of these structures occupy the S2" subsite (Figure 2).[22] In this way, our present work validates a novel molecular shape, a fused pyrrolidine iminopyrimidinone, that only occupies S1 and

S2'-S2", and thus achieves a similar overall profile with unique structural diversity. The discovery and characterization of compound **9** will be the central focus of this article.

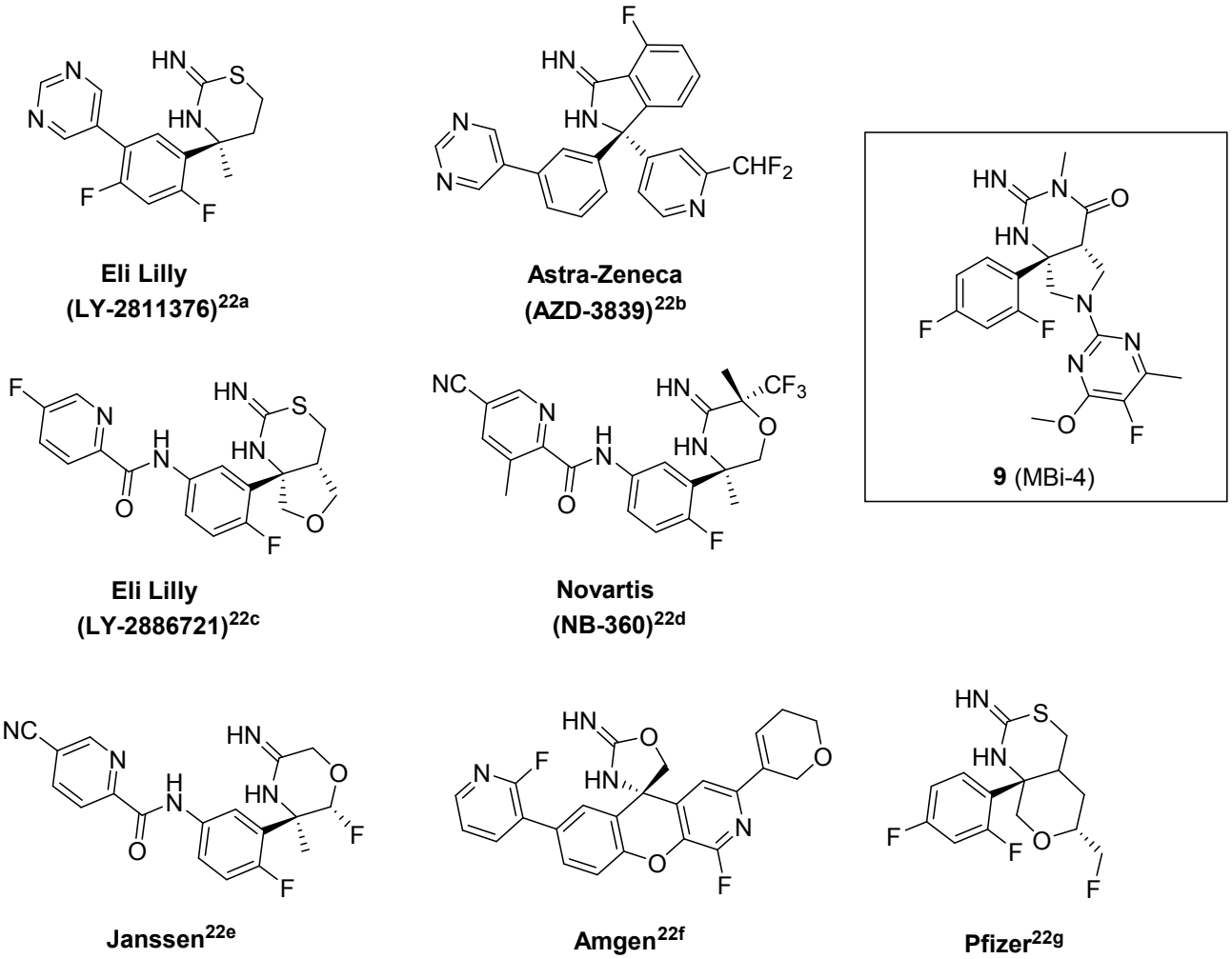

Figure 2: Structures of representative published BACE inhibitors that lower central Aβ in monkeys and/or dogs.

Chemistry

Synthetic routes to P1 thiophene analogs **10-17** are shown in Scheme 1. Bromothiophene core **26** was prepared following our previously described synthetic route[21] and was debrominated under standard hydrogenation conditions to provide thiophene **27** as a flexible intermediate. Re-bromination of compound **27** with *N*-bromosuccinimide (NBS) afforded isomeric bromothiophene **28** that was

subjected to palladium-mediated cyanation using $Zn/ZnCN_2$ followed by removal of the 2,2,2-trichloroethoxycarbonyl (Teoc) group with tetrabutylammonium fluoride (TBAF) to provide pyrrolidine

Scheme 1. Synthesis of P1 thiophene analogs 10-17[a]

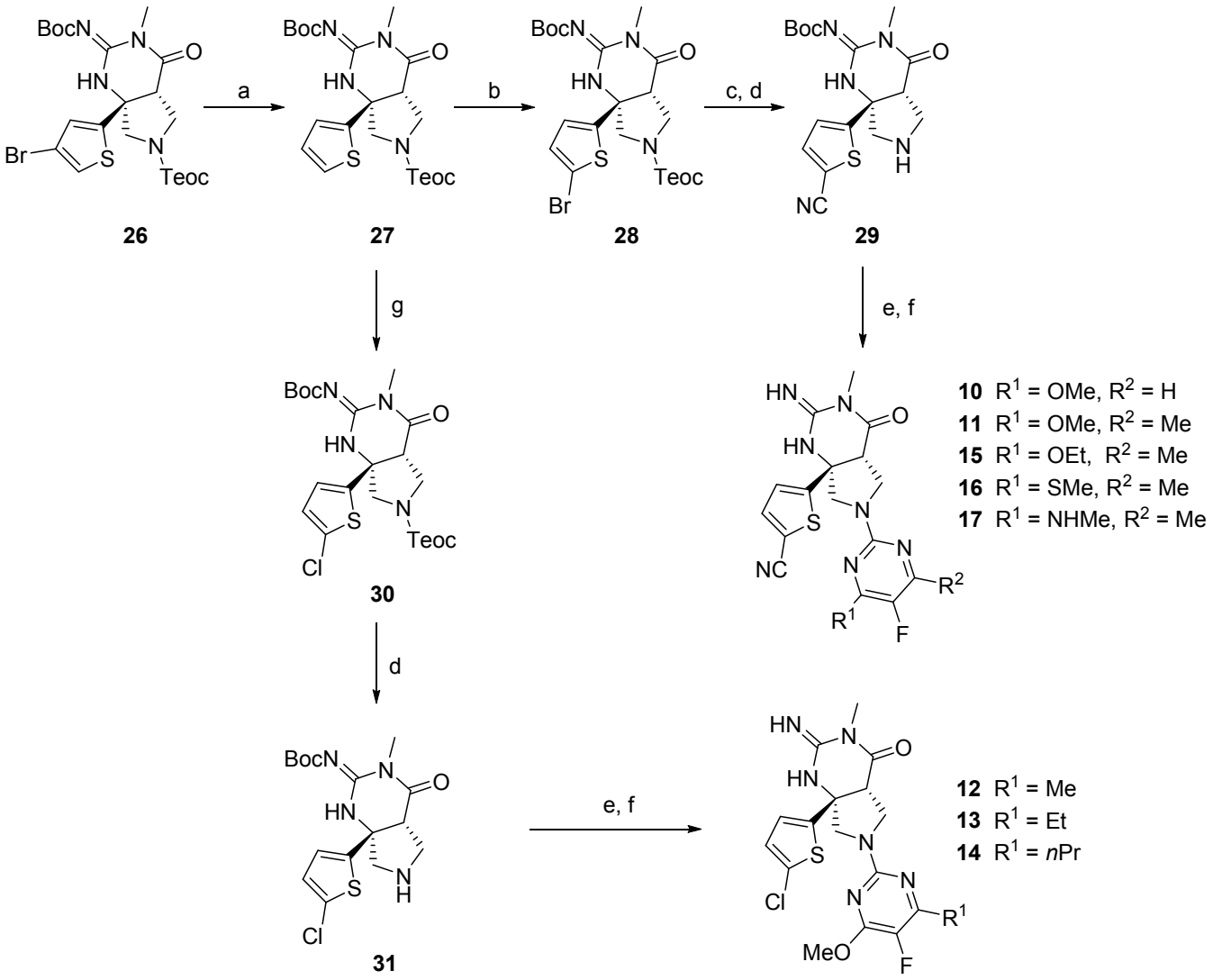

[a]Reagents and conditions: (a) 10% Pd/C, H_2, methanol, rt, 92%; (b) NBS, DMF, 60%; (c) $Zn(CN)_2$, Zn, $PdCl_2(dppf)•CH_2Cl_2$, DMA, then Et_3N, $(Boc)_2O$, CH_2Cl_2, 71%; (d) TBAF, THF, 80%; (e) heteroaryl halide, tris(dibenzylideneacetone)dipalladium(0), Na-O*t*Bu, (2-biphenylyl)di-*tert*-butylphosphine (JohnPhos), toluene, 65 °C, 30-80%; (f) TFA, CH_2Cl_2; (g) NCS, DMF, 75-80%.

29. To generate the analogous pyrrolidine with a P1 chlorothiophene **31**, intermediate **27** was chlorinated using *N*-chlorosuccinimide (NCS) to afford compound **30** that was subsequently treated with TBAF. Compounds **29** and **31** were used for preparation of compounds **10-17** in two steps – palladium-mediated *N*-heteroarylation with a variety of heteroaryl halides followed by treatment of the resulting products with TFA to remove the *tert*-butoxycarbonyl (Boc) protecting group.

Synthesis of compound **9** is depicted in Scheme 2 as a representative example for the approach to P1 phenyl analogs **18-22**. Commercially available nitrile **32** was condensed with aqueous glyoxylic acid using potassium carbonate, and product **33** spontaneously precipitated from the reaction mixture. Hydrolysis of the nitrile moiety of **33** using a mixture of sulfuric and formic acid produced, after dehydrative cyclization, anhydride **34**. In contrast to our previous efforts,[21] anhydride **34** was not hydrolyzed to the corresponding diacid but rather was used directly in the dipolar cycloaddition with commercially available *N*-benzyl-1-methoxy-*N*-((trimethylsilyl)methyl)methanamine **35.** After the cycloaddition reaction was complete, removal of the solvent and treatment of the crude residue with methanol resulted in precipitation of methyl ester **36** as a single regioisomer from solvolysis of the initial cycloaddition product. The carboxylic acid moiety of **36** was converted to an amine *via* diphenylphosphoryl azide (DPPA)-mediated Curtius rearrangement using 2-(trimethylsilyl)ethanol as the isocyanate trapping agent followed by unmasking the free amine by treatment with HCl to give intermediate **37**. Boc-protected iminopyrimidinone core **38** was formed by coupling between **37** and *t*-butyl *N*-[(methylamino)thioxomethyl]carbamate.[18] The enantiomers of compound **38** were separated using chiral HPLC to provide desired isomer **39** and its enantiomer **40**. Removal of the benzyl group of **39** followed by palladium mediated coupling of pyrrolidine **41** with 2-chloro-5-fluoro-4-methoxy-6-methylpyrimidine and subsequent treatment of the resulting intermediate with TFA provided compound **9**.

Scheme 2. Synthesis of 2,4-difluorophenyl analog 9[a] and related analogs 18-22.

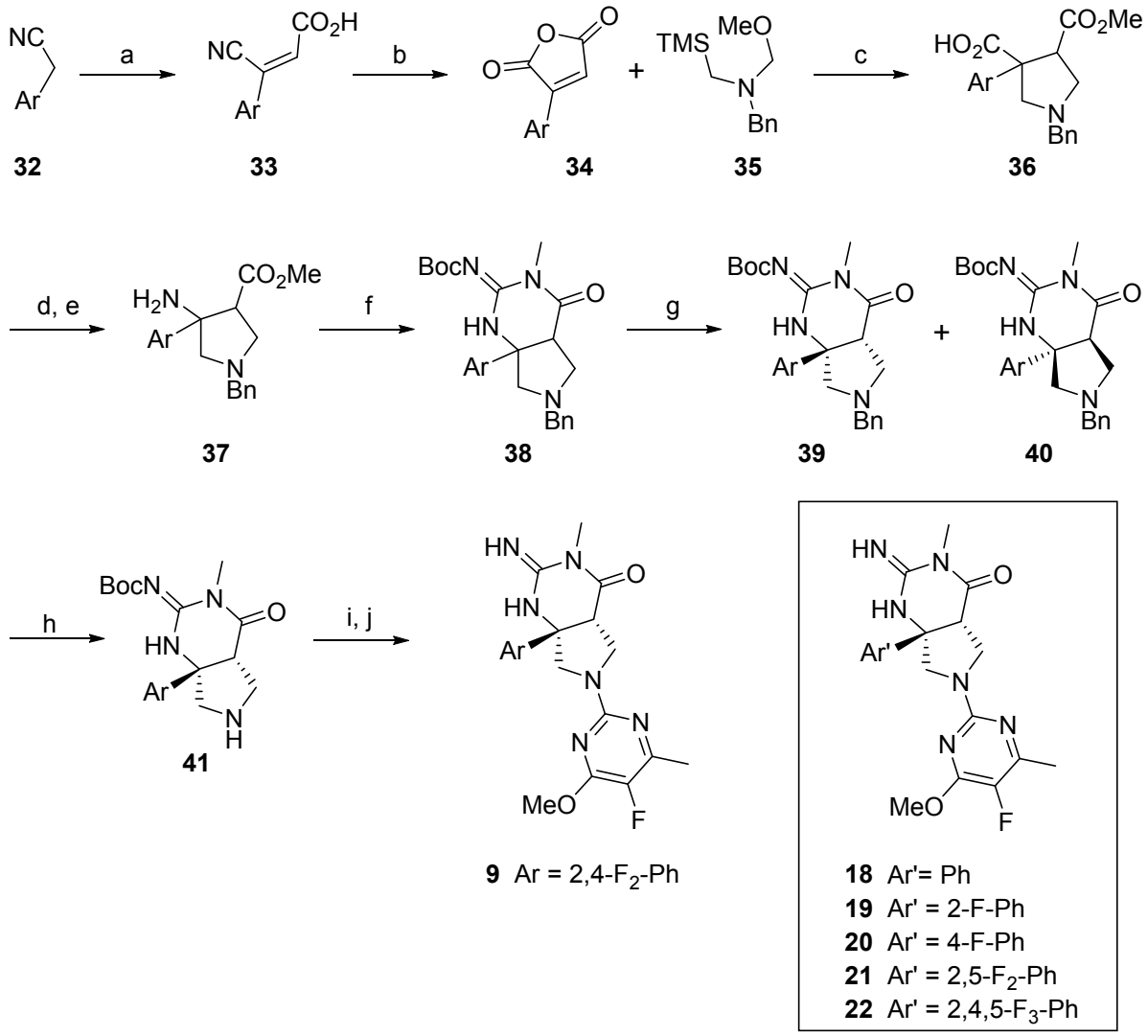

[a]Reagents and conditions: (a) glyoxylic acid (50% aqueous), K_2CO_3, MeOH, rt, 89%; (b) 7% concentrated H_2SO_4 in formic acid, 100 °C, 94%; (c) cat. TFA in THF, 0 °C to rt; concentration then dilution with MeOH, rt, 57%; (d) DPPA, Et_3N, toluene, 66 °C then acetic acid, TMS-ethanol, reflux, 48%; (e) 4N HCl in dioxane, rt; (f) *t*-butyl *N*-[(methylamino)thioxomethyl]carbamate, EDCI, DIEA, DMF, rt, 63%; (g) HPLC, AD column; (h) H_2, 20% $Pd(OH)_2$/C, MeOH, rt, 91%; (i) 2-chloro-5-fluoro-4-methoxy-6-methylpyrimidine, $Pd(OAc)_2$, Na-O*t*Bu, toluene, 2'-(di-*tert*-butylphosphino)-*N*,*N*-dimethyl-[1,1'-biphenyl]-2-amine, 120 °C; (j) TFA, DCM, 58%.

Preparation of analogs **23-25** required changes to the synthetic route due to perturbation of the stereoelectronics of the neighboring carbons imposed by 2,6-difluoro substitution. Scheme 3 shows this

modified synthetic route for compound **23**. Note that the pyrrolidine intermediates analogous to compound **46** en route to analogs **24** and **25** were made by a slightly different sequence as shown in Scheme 4 for intermediate **56**.

Scheme 3. Synthesis of 2,6-difluorophenyl analog 23[a]

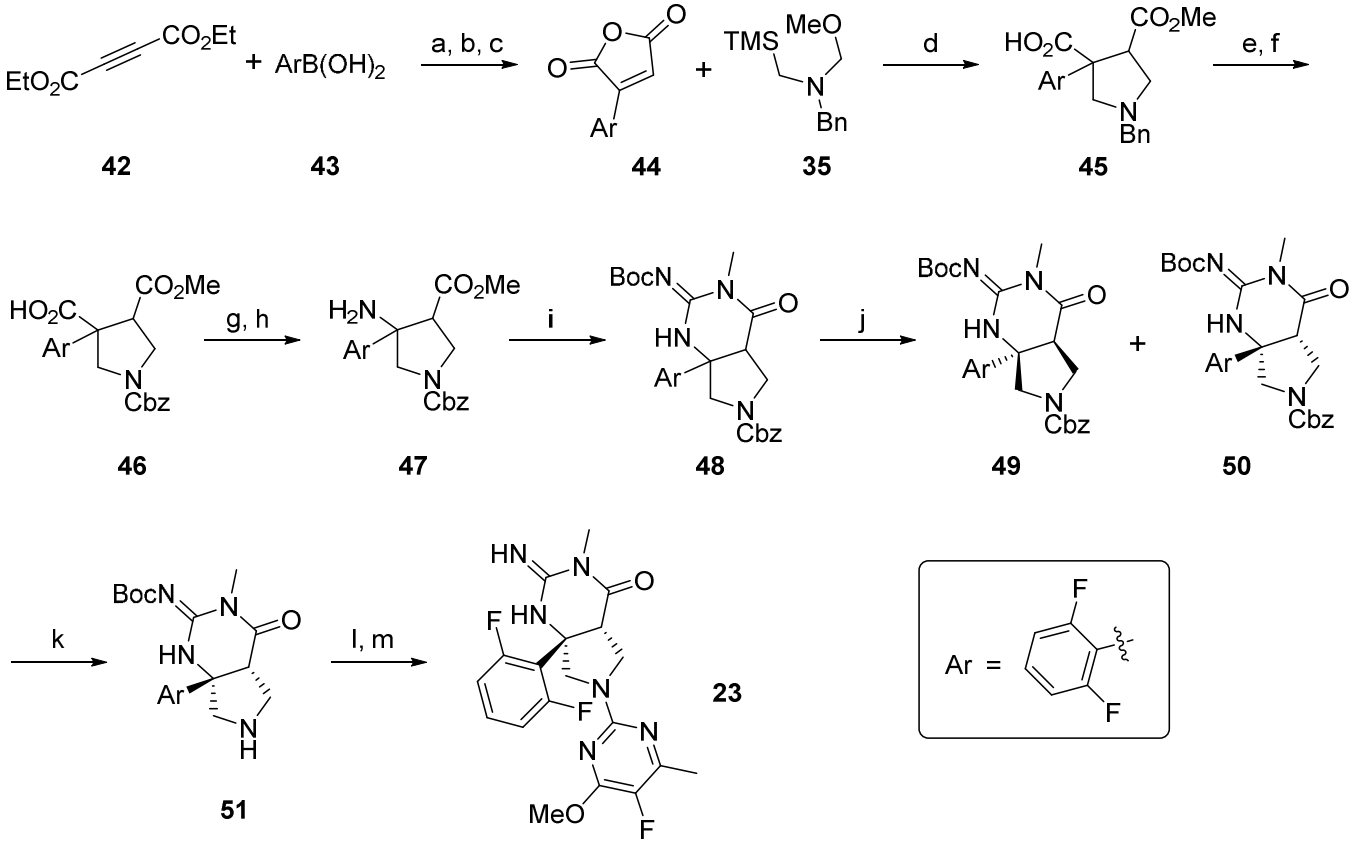

[a]Reagents and conditions: (a) $Pd(PPh_3)_4$, AcOH, dioxane, 80 °C, 34%; (b) LiOH•H_2O, THF, 40 °C; (c) acetic anhydride, 90 °C, 99%; (d) cat. TFA in THF, 0 °C to rt; concentration then dilution with pre-mixed MeOH/Et_3N, -60 °C to rt, 56%; (e) 20% $Pd(OH)_2$ on carbon, H_2, MeOH; (f) CbzCl, Et_3N, MeOH, THF, 64% from **45**; (g) DPPA, Et_3N, toluene, then TMS-ethanol, 120 °C, 67%; (h) 4N HCl in dioxane, rt; (i) *t*-butyl *N*-[(methylamino)thioxomethyl]carbamate, EDCI, DIEA, DMF, rt, 57%; (j) HPLC, AD column; (k) 20% $Pd(OH)_2$ on carbon, H_2, MeOH, rt, 98%; (l) 2-chloro-5-fluoro-4-methoxy-6-methylpyrimidine, tris(dibenzylideneacetone)dipalladium(0), Na-O*t*Bu, (2-biphenylyl)di-*tert*-butylphosphine (JohnPhos), toluene, 65 °C, 46%; (m) TFA, DCM, 63%.

Scheme 4. Synthesis of pyrrolidine intermediate en route to 2,3,6-trifluorophenyl analog 24[a]

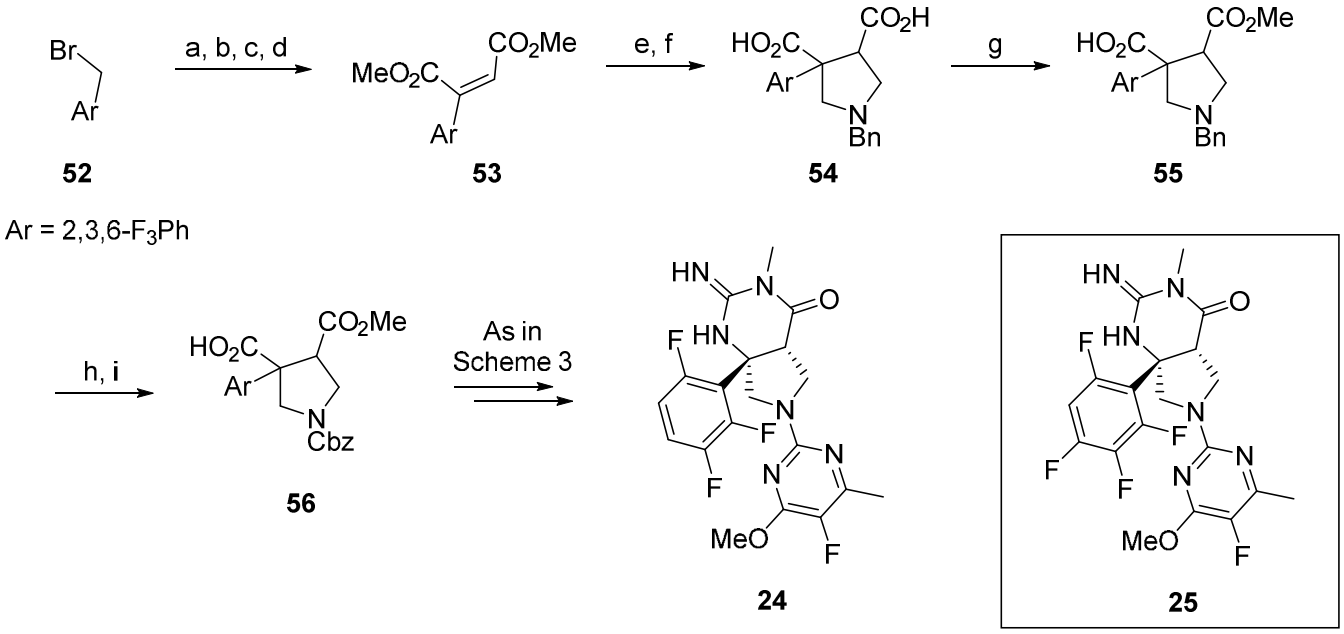

[a]Reagents and conditions: (a) NaCN, EtOH, H_2O, reflux, 79%; (b) glyoxalic acid monohydrate, K_2CO_3, MeOH; (c) 10% conc. H_2SO_4 in formic acid, reflux; (d) 5% conc. H_2SO_4 in MeOH, reflux, 41%; (e) *N*-benzyl-1-methoxy-*N*-((trimethylsilyl)methyl)methanamine, cat. TFA, THF, rt, 100%; (f) 15% conc. H_2SO_4 in water, reflux; (g) Ac_2O, 90 °C, then, MeOH and Et_3N, -78 °C; (h) $Pd(OH)_2$, MeOH, rt; (i) CbzCl, Et_3N, THF, rt, 79%.

Results and Discussion

Our previous SAR studies generated three optimized lead compounds **6**-**7**,[21] and **8** from iminopyrimidinone series with BACE1 K_i values of 3.5, 5.6 and 0.9 nM respectively (Figure 3). Despite their similar structures and affinities, X-ray co-crystal structures with BACE1 showed that these molecules each exhibit unique binding features in S2'-S2" (Figure 3(a)). The fluoropyrimidine moiety of compound **6** binds in an open hydrophobic space near S2' and establishes a hydrogen bonding network with Trp[76] through a highly conserved water molecule in a sub-pocket we have termed S2". While the pyridine substituent of analog **7** overlays with the pyrimidine of compound **6** very well, it projects the cyano substituent into S2" to displace the conserved water molecule and forms a direct hydrogen bond with Trp[76]. In sharp contrast to the two modes above, the methoxypyridine moiety of **8**

shifted roughly 2 Å relative to the other analogs to displace two conserved waters and displaying the methoxy group deep in the S2" binding pocket.

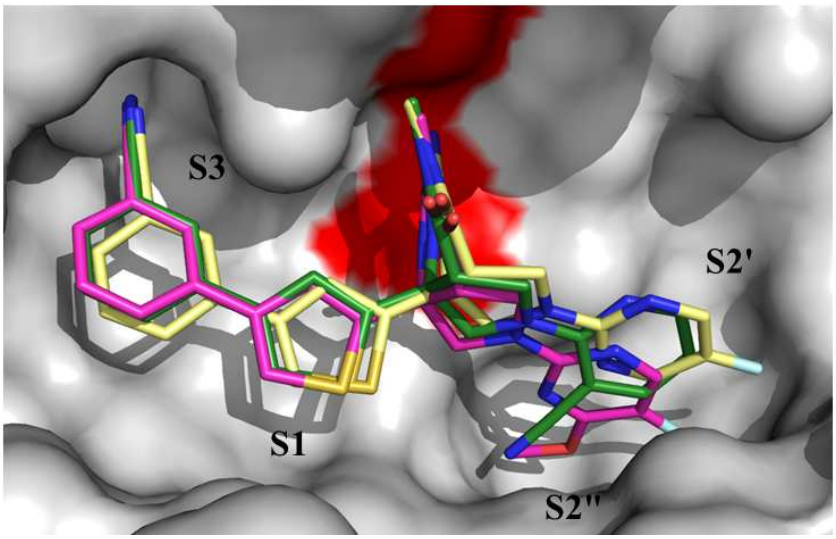

(a)

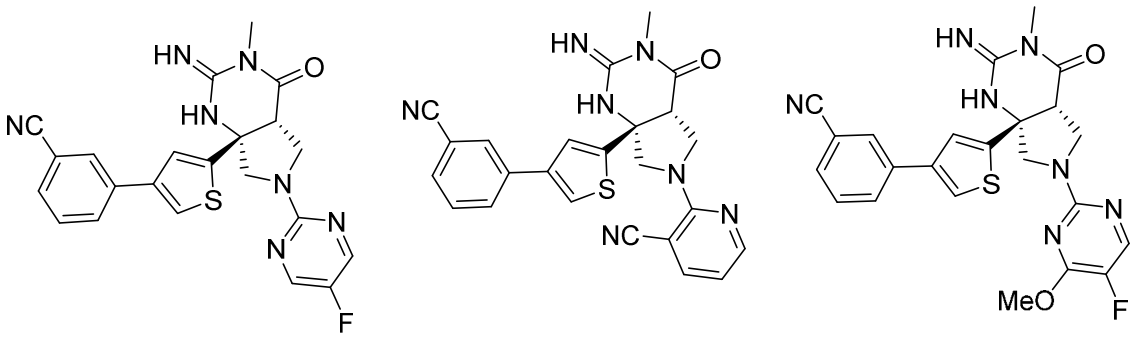

	6	**7**	**8**
BACE1 K_i	4 nM	6 nM	1 nM
MW	447.5 Da	453.5 Da	477.5 Da
cLogP	2.58	2.79	3.31
PSA	109 Å^2	120 Å^2	118 Å^2
3A4 IC_{50} (pre)	1.2 μM	>30 μM	2 μM
CatD/BACE1	93	39	95

(b)

Figure 3: (a) Superimposed X-ray conformation of iminopyrimidinone **6** (yellow, PDB ID code: 5hd0), **7** (green, PDB ID code: 4h3g), **8** (magenta, PDB ID code: 5hdu) in the active site of BACE1 with red surface showing the location of catalytic aspartic acids. (b) Structures of **6**, **7** and **8** with their respective BACE1 K_i, CYP3A4 IC_{50} (pre), CatD/BACE1 selectivity and calculated properties.

The different arrangements of the pyridine and pyrimidine moieties offered several potential strategies for further optimization of the overall inhibitor profiles. At the outset, however, we were cognizant that optimization of **6**, **7** and **8** (Figure 3(b)) should avoid the incorporation of additional molecular weight and lipophilicity since this could result in profiles unsuitable for a CNS agent and would likely only exacerbate critical off target liabilities (e.g. *h*ERG). Therefore our strategy was to remove the P3 cyanophenyl moiety to afford lower molecular weight scaffolds that occupy two binding sites (S1 and S2''), from which we could pursue SAR to rescue any intrinsic potency loss while fine tuning physicochemical properties (cLogP, PSA) into CNS drug-like ranges. Such inhibitors would be structurally differentiated from the majority of optimized amidine-based analogs that occupy the S1-S3 pockets.[22a-f,23] Additionally we envisaged that optimization based on **6** and **8** would necessitate modification of their fluoropyrimidine moieties. It was hypothesized that the time-dependent CYP3A4 inhibition observed with **6** and **8** (Figure 3(b)) was a result of bioactivation of the fluoropyrimidine moiety to generate a reactive intermediate. Evidence for this was provided by incubation of **6** with recombinant CYP3A4, supplemented with glutathione, which led to the formation of a product of *m/z* 751.2104 corresponding to a glutathione adduct of **6** with concomitant loss of fluoride.

Implementation of this strategy using **6** and **7** as starting points failed to provide an inhibitor with an acceptable overall profile. On the other hand, compound **8** presented some potential advantages as a starting point including higher BACE1 affinity and similar or better selectivity for BACE1 over cathepsin D (CatD) compared to **6** and **7**. The importance of achieving substantial selectivity for BACE1 over CatD has been highlighted by the recent report of ocular toxicity and neurodegeneration in rats that was attributed to CatD inhibition with the modestly selective BACE1 inhibitor LY-2811376.[22a]

Truncation of the P3 cyanophenyl group of compound **8** to P1 cyanothiophene analog **10** led to a 40-fold drop in BACE1 affinity (Table 1). Introduction of a methyl group at the 6-position of the pyrimidine gave compound **11** resulting in a 4-fold gain of BACE1 affinity. Replacement of the P1 5-cyano substituent of **11** with chloro (**12**) resulted in similar affinity and cellular potency for Aβ_{40} lowering. On the other hand, further increase in lipophilicity resulting from replacement of the pyrimidine methyl substituent of **12** with ethyl (**13**) or n-propyl (**14**) was detrimental to cellular potency. The X-ray crystal structure of **11** complexed with BACE1 showed that truncation and subsequent pyrimidine substitution did not affect the overall binding mode of this series. The methoxy group of the pyrimidine remains deep in the S2" binding pocket while the methyl group projects toward the S2' binding site as designed (Figure 4). Selectivity for BACE1 over CatD for the truncated analogues was generally maintained or eroded relative to **8**, with the exception of **15** which appeared to be highly BACE1 selective (Table 1). In the absence of a crystal structure of **15** and its analogues in complex with CatD, a convincing explanation for the observed high selectivity of **15** is not readily apparent. A recent publication disclosing inhibitors that bind a region of BACE1 similar to that for the inhibitors described herein attributed the observed CatD selectivity to be a result of interactions between the inhibitors and Tyr^{78} and Trp^{40} of CatD.[22g]

Table 1. SAR investigation of truncated thiophene analogs.[a]

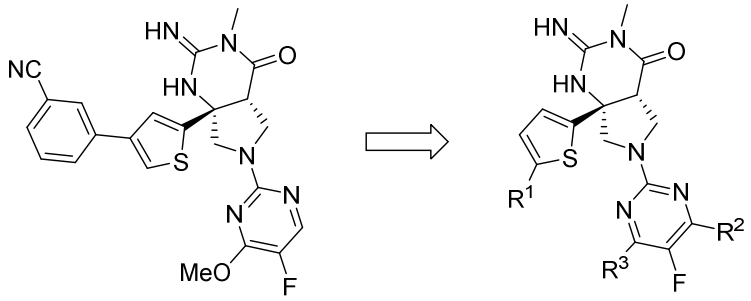

8 **10-17**

Cpd	R^1	R^2	R^3	MW (ClogP)	BACE1 K_i (nM)	HEK293 Aβ_{40} IC_{50} (nM)	LE	CatD / BACE1
8				468 (2.8)	1.4	18	0.35	95
10	CN	H	OMe	401 (1.0)	57	238	0.35	93
11	CN	Me	OMe	416 (1.5)	15	40	0.46	39
12	Cl	Me	OMe	435 (2.7)	10	51	0.39	70
13	Cl	Et	OMe	439 (3.2)	11	203	0.39	ND
14	Cl	*n*Pr	OMe	453 (3.8)	15	190	0.35	18
15	CN	Me	OEt	430 (2.0)	48	361	0.33	>2000
16	CN	Me	SMe	432 (2.0)	45	36	0.34	5.2
17	CN	Me	NHMe	414 (1.6)	336	157	0.30	66

[a]Protocols for determination of inhibitor K_i values against purified human BACE1 and Cathepsin D, as well as for cellular BACE1 IC_{50} values, have been previously described.[16]

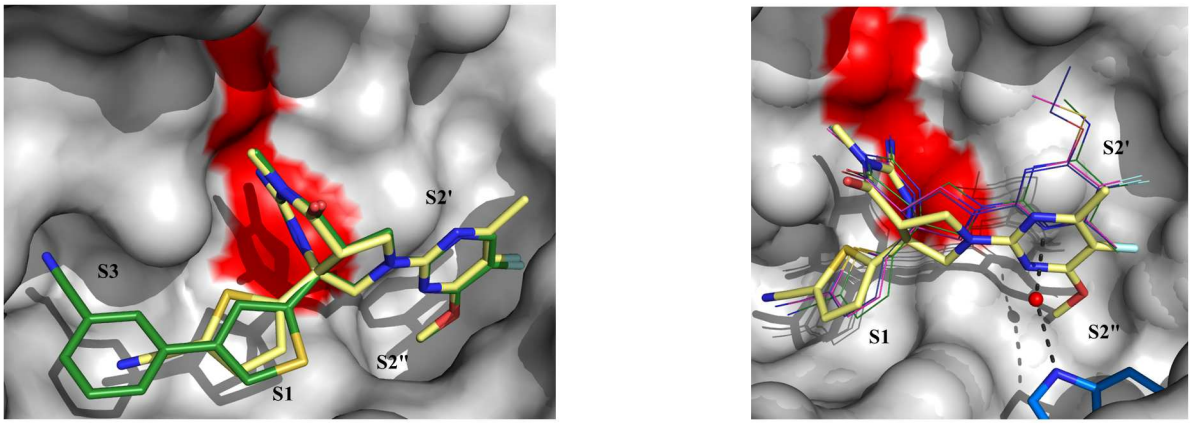

(a) (b)

Figure 4: (a) Superimposition of X-ray crystal structures of **11** (yellow, PDB ID code: 5hdv) and **8** (green, PDB ID code: 5hdu) complexed with BACE1. Red surface represents the catalytic dyad Asp^{32} and Asp^{228}. (b) Overlay of X-ray crystal structures of **11** (yellow, PDB ID code: 5hdv), **15** (blue, PDB ID code: 5hdx), **16** (purple, PDB ID code: 5hdz) and **17** (green, PDB ID code: 5he5). The red ball represents the bridging water molecule between the Trp^{76} and the nitrogen of the pyrimidine of **15**, **16** and **17**. Pyrimidine moieties of **15**, **16** and **17** have shifted almost 1.9 Å towards S2' binding site.

To probe if methoxy was optimal for binding in S2", the methoxy group of **11** was homologated to the ethoxy analog **15** which resulted in a three-fold loss in BACE1 affinity and a similar loss of cellular potency. We next examined the isosteric aminomethyl and thiomethyl replacements. Thiomethyl substitution was tolerated with affinity similar to that of the ethoxy analog (**16**, BACE1 K_i = 45 nM). In contrast, aminomethyl analog **17** displayed a significant drop in affinity (BACE1 K_i = 336 nM). Interestingly, the X-ray structures of **15, 16** and **17** complexed with BACE1 showed that the pyrimidine moiety had flipped to orient the ethoxy, thiomethyl and aminomethyl moieties toward the S2' binding pocket and that the pyrimidine ring had shifted from the S2" binding site by approximately 1.9 Å, engaging in an interaction with Trp^{76} through conserved water molecules mimicking the binding modes of compound **6** (Figure 4(b)). Whereas the in-plane *anti*-oriented methoxy group of the pyrimidine ring of **11** is positioned optimally in the S2" pocket, larger groups such as ethoxy and

thiomethyl (*e.g.* **15** and **16**), or groups that lack the energetics to adopt preferentially the *anti*-orientation such as the aminomethyl group (*e.g.* **17**) occupy the relatively larger S2' binding site.

S1 SAR with optimized S2'-S2'' moiety

The SAR explorations described above demonstrated that truncation from S3 and optimization of the substituents in S2" and S2' could generate potent, ligand-efficient analogs relative to their higher molecular weight precursors. In fact, the optimal S2'-S2" substituent, 4-methoxy-5-fluoro-6-methylpyrimidine present in analogs **11** and **12** imparted excellent affinity with minimal (methyl) occupancy of S2', and both of these analogs gratifyingly showed reduced time-dependent inhibition of CYP3A4 compared to starting point **8** (IC_{50} 2 μM for **8** vs. 24 μM and 18 μM for **11** and **12** respectively). We attribute the reduced time-dependent CYP3A4 inhibition of **11** and **12** to the increased steric demand of the newly introduced methyl substituent reducing the rate oxidation of the pyrimidine moiety and/or redirecting metabolism to the methyl group itself.

Given that the S1 thienyl moiety was originally installed to provide an optimal vector for the now absent aryl substituent into the S3 pocket, we next chose to replace this group with phenyl in combination with the optimized S2'-S2" pyrimidine substituent. In this regard, compound **18** was well tolerated with a BACE1 K_i of 36 nM and whole cell potency of 58 nM (Table 3). A series of mono- and polyfluorinated phenyl analogs was also prepared to assess SAR related to in vitro potency, selectivity, and rat PK parameters. As shown in Table 3, introduction of fluorine to the P1 phenyl was generally beneficial, imparting improved K_i values (e.g. **9**, **19-22**). The improvement in potency may be due to general hydrophobic contacts within the lipophilic S1 site, or may be driven by electrostatic interactions of the fluorine with the phenyl rings of Trp^{115} and with the hydroxyl group of flap Tyr^{71} as suggested by the X-ray co-crystal structure of the 2,4-difluorophenyl analogue **9** (Figure 5(a)).[24] The

Table 3. SAR investigation of fluorophenyl substitution in the presence of the 4-methoxy-5-fluoro-6-methylpyrimidinyl substituent.[a]

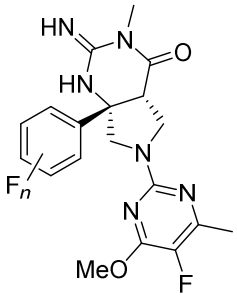

Cpd	R[1]	MW (ClogP)	BACE1 K_i (nM)	HEK293 $A\beta_{40}$ IC_{50} (nM)	CatD/ BACE1	C_B (μM)[b]	B/P	CYP3A4 (preincubation, μM)
18	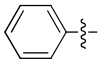	384 (2.3)	36	58	349	ND	ND	>30
19	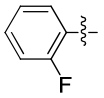	402 (2.5)	6	17	143	0.074	0.7	>30
20	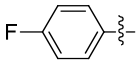	402 (2.5)	7	16	354	0.32	0.9	34.1
9	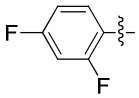	420 (2.6)	5	14	458	0.072	1.1	>30
21	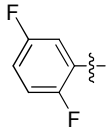	420 (2.6)	9	28	158	0.056	0.7	>30
22	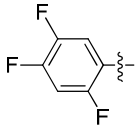	438 (2.7)	8	35	446	ND	NA	>20
23	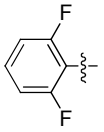	420 (2.6)	20	49	636	ND	ND	>20
24	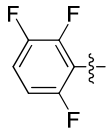	438 (2.7)	53	234	151	0.088	0.4	>20
25	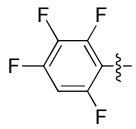	456 (2.8)	30	93	99	0	NA	~30

[a]Protocols for determination of inhibitor K_i values against purified human BACE1 and cathepsin D, as well as for cellular BACE1 IC_{50} values, have been previously described.[16] [b]Concentration in brain homogenate 6h post 10 mpk PO dosing.

exception to the potency improvements with fluorine addition are the 2,6-difluoro-containing analogs **23**-**25**. These analogs are all slightly less active than their 2-fluoro-6-proteophenyl counterparts (analogs

9, **19-22**), possibly due to a weakly-negative interaction with carbonyl of Gly^{230} and carbonyl of the side chain carboxylic acid of Asp^{32} (Figure 5(b)).

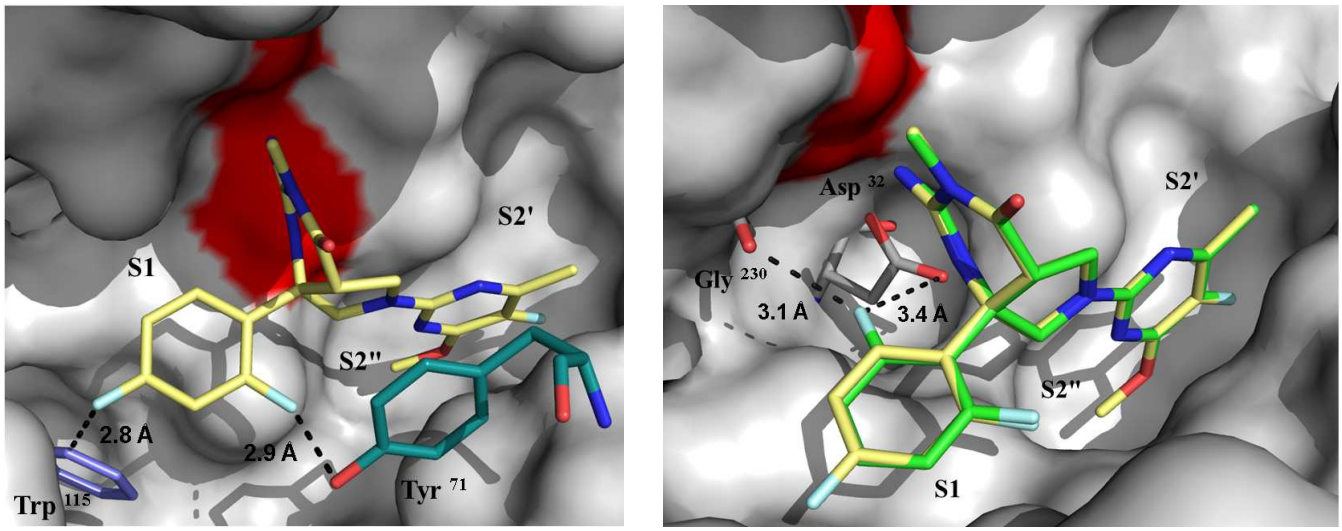

(a) (b)

Figure 5: (a) X-ray crystal structure of **9** complexed with BACE1. The hydroxyl moiety of Tyr^{71} of the flap is 2.9 Å away from the 2-fluorine of 2,4-difluorophenyl group of compound **9**. (b) Superimposition of X-ray crystal structures of **9** (yellow, PDB ID code: 5he7) and a racemic sample of **23** (green, PDB ID code: 5he4) complexed with BACE1. The 6-fluorine of the bound enantiomer of **23** is 3.1 Å away from the backbone carbonyl of Gly^{230} and is 3.4 Å away from the carbonyl of the side chain carboxylic acid of Asp^{32}.

Importantly, in all cases, the addition of fluorine did not significantly erode the cell Aβ_{40} IC_{50} values relative to the K_i values of these analogs, and compounds **9**, **19** and **20** showed cell IC_{50} values of <20 nM. In addition, all of these analogs showed at least 100-fold selectivity over CatD and did not show significant inhibition of CYP 3A4 under preincubation conditions. Of these, the 2,4-difluorophenyl analogue **9** was selected for further profiling based on its favorable overall profile with respect to BACE1 affinity, cell potency and 460-fold selectivity over CatD.

Compound **9** displayed good selectivity for BACE1 over the human aspartic proteases pepsin, (>20000x), renin (6820x) and cathepsin E (648x), but was not selective versus the closely related

BACE1 homolog BACE2 (K_i = 2.7 nM). Expressed predominantly in the periphery, BACE2 processes the melanocyte structural protein PMEL17 required for proper pigmentation in rodents.[25] BACE2 is also expressed in pancreatic β-cells and loss of BACE2 function has been associated with improved glucose homeostasis.[26] While knowledge of BACE2 mediated biological processes continues to evolve, current understanding mitigates concerns related to BACE2 inhibition for development of a therapeutic agent. In a counterscreen of a panel of human receptors, enzymes and ion channels, **9** did not show significant off target activity with the exception of histamine H2 (K_i = 4.9 μM), melatonin MT1 (K_i = 2.9 μM), and motilin (K_i = 19 μM) receptors.

Table 4. Rat, dog and monkey pharmacokinetic parameters of **9**

Species	Dose (mg/kg)[a]	$AUC_{(0-\infty)}$ (μM.hr)[a]	C_{max} (μM)[a]	%F	Hep. Cl_{int} μL/min/10^6 cells	In vivo clearance mL/min/kg[b]	$V_{d,ss}$ (L/kg)[b]	$t_{1/2}$ (hr)[b]
Rat	3	0.30	0.1	19	53	92	9.0	1.1
Dog	3	0.39	0.19	8.2	73	35	3.6	2.2
Monkey	3	2.6	0.49	33	48	15	5.7	7.3

[a]Oral. [b]Intravenous (3 mg/kg for rat and 1 mg/kg for dog and monkey).

Compound **9** did not significantly inhibit human CYP's 1A2, 2C8, 2C9, 2C19, 2D6 and 3A4 at concentrations below 20 μM and thus has minimal risk of interaction with drugs that are metabolized by the major human CYPs, demonstrating a marked improvement over its progenitor **6**. Inhibition of the *h*ERG channel by **9** (IC_{50} = 1.9 μM) was also reduced relative to **6**.

The pharmacokinetic parameters of **9** are shown in Table 4. Oral bioavailability of **9** was low in rats and dogs and moderate in monkeys, consistent with the high Cl_{int} observed in hepatocytes of the respective species. In vivo total clearance exceeded liver blood flow in rats and dogs, indicating that

clearance pathways other than hepatic extraction contribute to total clearance. In this regard, **9** was unstable in rat and dog plasma suggesting that its plasma instability may constitute a significant extra-hepatic clearance pathway in these species. In cynomolgus monkeys, total in vivo clearance of **9** was moderate and in concert with the moderate volume of distribution resulted in higher plasma exposure and a longer half-life in vivo. The compound achieves substantial total brain concentrations in rats and

Dose (mg/kg, PO)	C_P (nM)[b]	C_{CSF}(nM)	C_B (nM)[c]
0.3	5.6	<bloq[a]	3.0
1	17.53	<bloq[a]	13.5
3	121.2	<bloq[a]	56.3
10	770.4	5.4	346.9
30	2981	26.1	1781.1
100	8805	80.7	4043
300	14186	119.8	5018

[a]bloq; below limit of quantitation (0.6 nM).
[b]Plasma concentration. [c]Brain concentration

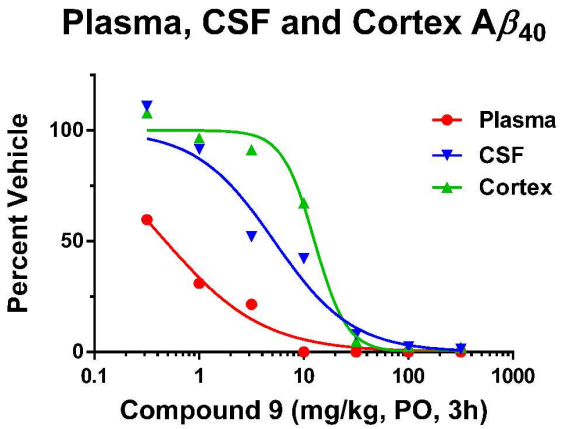

(a) **(b)**

Figure 6. (a) Measured total concentration of **9** in plasma (C_P), CSF (C_{CSF}) and brain (C_B) of rats at doses ranging from 0.3 mg/kg to 300 mg/kg. (b) Effect of acute oral administration of compound **9** on the reduction of plasma, CSF and cortical Aβ_{40} levels in rats.

monkeys (brain/plasma ratio of 0.8 and 3.2, respectively). The improved brain penetration of **9** compared to **6** (brain / plasma ratio of 1.1 versus 0.1,[21] respectively) is consistent with the reduction in calculated PSA achieved during optimization (PSA 94 Å^2 vs. 109 Å^2, respectively). While instability of **9** in plasma from rat, dog and monkey precluded accurate determination of plasma protein binding values, the compound is more stable in human plasma (95% bound). In human hepatocytes **9** exhibited low intrinsic clearance (1.8 µL/min/10^6 cells), in contrast with the high hepatocyte clearance observed in rat, dog and monkey hepatocytes (Table 4).

Compound **9** was evaluated to assess its ability to lower Aβ_{40} in the plasma, brain and CSF of rats (Figure 6). Dose related increases in exposure of **9** in plasma, brain and CSF was seen across the dose range of 0.3 – 300 mg/kg, and dose responsive lowering of Aβ_{40} was observed in all three compartments. A dose of 0.3 mg/kg of **9** lowered Aβ_{40} in plasma to 40% of the control levels corresponding to an ED_{50} for Aβ_{40} lowering of 0.5 mg/kg in plasma. On the other hand, potency for CSF and cortex Aβ_{40} lowering was considerably shifted rightward with ED_{50s} of 5.2 mg/kg and 12.7 mg/kg respectively. Notably, levels of **9** in the CSF were below the limit of quantitation at the 3 mg/kg dose, a dose at which significant CSF Aβ_{40} lowering was observed. Consistent with this observation, **9** was determined to be a rat Pgp substrate in an MDCK cell line overexpressing MDR1 (efflux ratio >30; P_{app} (41×10^{-6} cm/s) indicating that CSF levels of **9** cannot be considered a reliable predictor of its free brain concentration.[27]

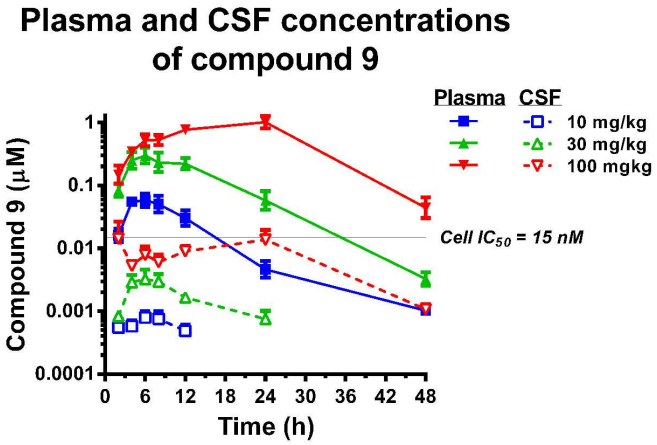

(a)

Dose (mg/kg)	10	30	100
	Plasma		
$AUC_{0\text{-}48h}$ (µM.h)	0.608	4.11	22.9
C_{max} (µM)	0.067	0.34	1.14
T_{max} (h)	5.0	7.0	20.0
	CSF		
$AUC_{0\text{-}48h}$ (µM.h)	0.0046	0.035	0.304
C_{max} (µM)	0.0009	0.0046	0.0234
T_{max} (h)	6.0	6.0	34.0

(b)

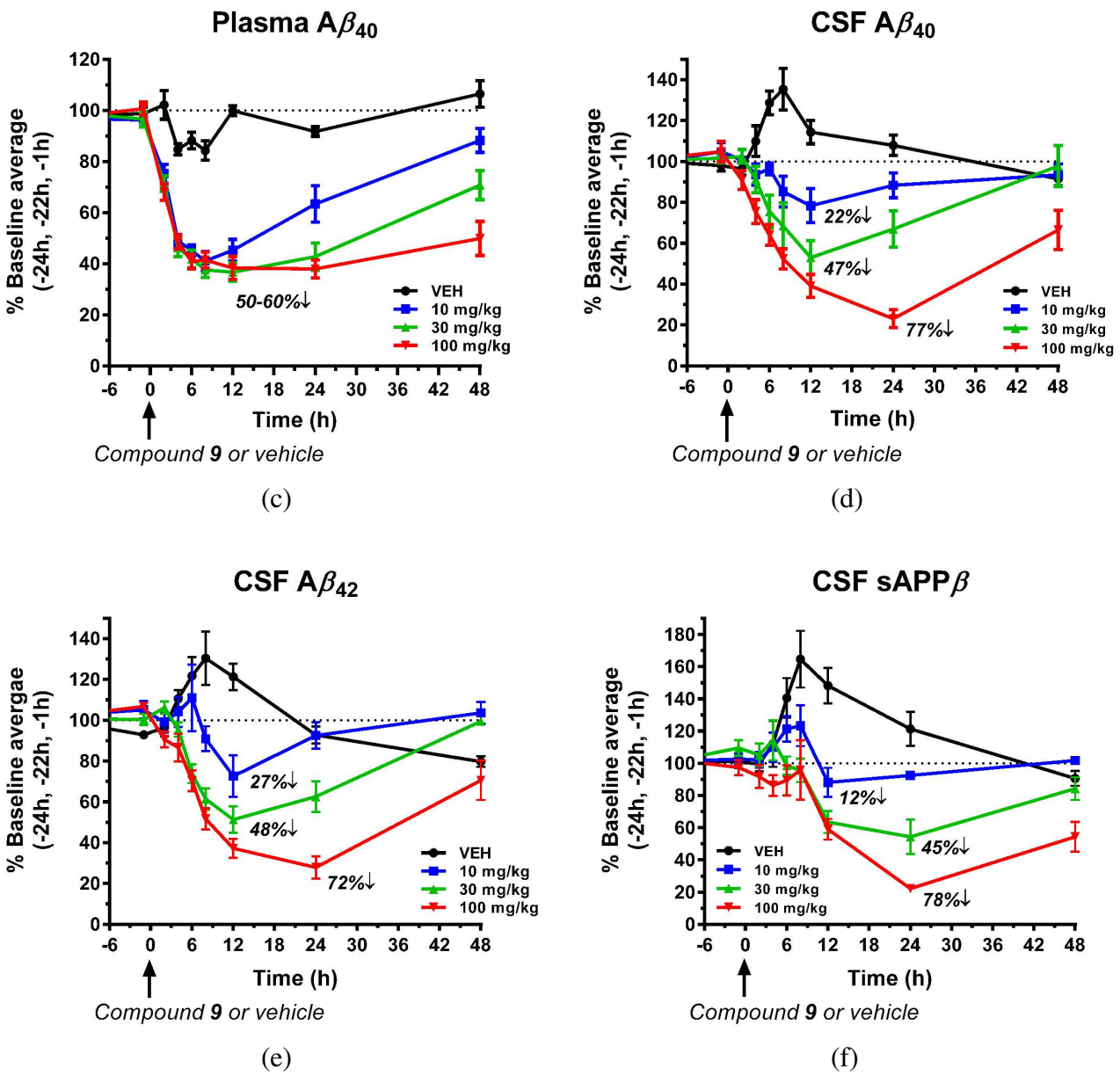

Figure 7: Acute PK/PD profile of compound **9** in cisterna magna ported rhesus monkeys. Plasma and CSF samples were collected at 2, 4, 6, 8, 12, 24 and 48 h after oral administration of **9** (10, 30 or 100 mg/kg) and analyzed for both compound concentrations and Aβ_{40} levels. (a) Plasma and CSF concentrations of **9** over time. (b) Pharmacokinetic parameters of **9**. (c) Plasma Aβ_{40} levels. (d) CSF Aβ_{40} levels. (e) CSF Aβ_{42} levels. (f) CSF sAPPβ levels.

The pharmacodynamic profile of **9** was also determined in non-human primates. Single doses of compound **9** (10, 30, and 100 mg/kg) were orally administered to cisterna magna ported rhesus monkeys enabling evaluation of its effect on the temporal dynamics of BACE1-related biomarkers in CSF and

plasma. Plasma and CSF samples were collected at 2, 4, 6, 8, 12, 24 and 48 h post dose to analyze compound and Aβ_{40} levels. In addition, Aβ_{42} and sAPPβ were analyzed at each time point in the samples from CSF. A dose dependent increase in exposure of **9** was observed in plasma and CSF (Figure 7(a)). Correspondingly, dose and time dependent reduction of CSF Aβ_{40} was observed with profound peak reduction (-77% relative to baseline) observed at 24 h following the high dose (Figure 7(d)). The maximum lowering of plasma Aβ_{40} at each dose was not differentiated, with apparent plateauing at 50-60% reduction as a result of the limited window of quantification by the plasma Aβ_{40} assay. However, a dose-dependent effect on the duration of plasma Aβ_{40} inhibition was observed which correlated with plasma exposures of **9** (Figure 7(c)). Peak reductions of CSF Aβ_{40} occurred at time points that were significantly delayed relative to the timing (T_{max}) of the plasma and CSF C_{max} concentrations of **9**, with the delay (~6 h) more pronounced at the lower doses (cf. Figures 7(a) and 7(d)). Reductions of Aβ_{42} and sAPPβ in the CSF followed a temporal pattern very similar to that of Aβ_{40} (Figures 7(e) and 7(f)). This hysteresis effect is likely related to the kinetics of central Aβ turnover and transit to the CSF from within the brain.[28]

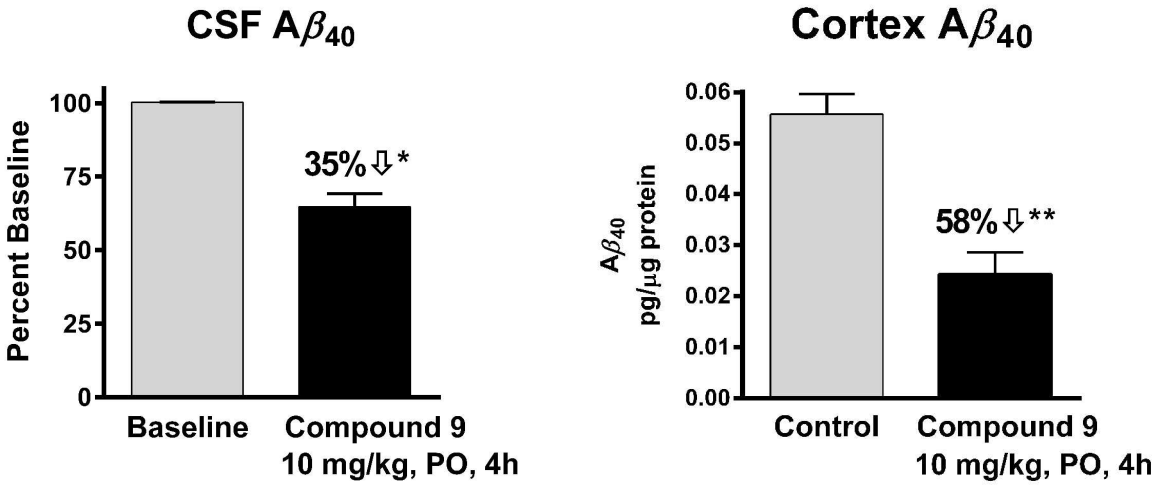

Figure 8. Acute effect of compound **9** (10 mg/kg) on CSF and cortical Aβ_{40} levels in cynomolgus monkeys (*p = 0.0014, **p < 0.0007).

The acute effect of **9** on the reduction of CSF and cortex Aβ_{40} was investigated in cynomolgus monkeys (Figure 8). Acute oral administration of **9** at 10 mg/kg resulted in 58% reduction of Aβ_{40} in cortex compared with the vehicle control group when evaluated at 4 h post dose. Interestingly, CSF Aβ_{40} reduction (35% relative to control) was not as pronounced as that observed in cortex at the same time point.

The greater reduction of cortex Aβ_{40} compared to CSF Aβ_{40} at the 4 h time point is thought to be a manifestation of the dynamics of Aβ_{40} transit and turnover under the conditions of acute administration of **9**. A close temporal relationship between BACE1 inhibition of Aβ_{40} synthesis and the magnitude of Aβ_{40} inhibition would be expected in cortex where Aβ_{40} is directly produced. In contrast, the degree of reduction of Aβ_{40} in the CSF under non-steady state conditions of acute inhibitor administration is dependent on the kinetics of Aβ_{40} clearance from CSF and of transit of newly synthesized Aβ into the CSF compartment from the primary sites of synthesis in the brain.[28] This hypothesis is consistent with the observed delay to maximum CSF Aβ_{40} lowering of 12-24 h post dosing in rhesus monkeys (Figure 7(d)).

Conclusions

Design and development of potent BACE1 inhibitors for advanced clinical studies has been challenging due to the intrinsic nature of the BACE1 active site and the localization of the enzyme within intracellular compartments of the brain. To achieve high affinity, inhibitors require polar functionality to interact with the active site catalytic aspartic acids complemented by lipophilic groups that bind in the adjacent specificity pockets. Successful inhibitor development requires an appropriate balance of properties to achieve cell and brain penetration while minimizing off target liabilities. Our earlier work employing the novel bicyclic iminopyrimidinone scaffold clearly illustrated these

challenges, resulting in the potent BACE1 inhibitor **6** which suffered from significant CYP3A4 and *h*ERG inhibition, and sub-optimal brain exposure. Using **6** as a starting point, improvement of the ancillary profile and CNS properties was achieved by truncation of the P3 moiety and optimization of the pyrimidine moiety binding in the S2'-S2'' region, delivering **11**. Subsequent optimization of the P1 aryl group of **11** to improve affinity and selectivity delivered 2,4-difluorophenyl analogue **9** which is structurally diverse from our previously reported S1-S3 binding inhibitors and afforded robust central Aβ reduction in rats and monkeys.

EXPERIMENTAL SECTION

Procedures for X-ray crystallography, aspartyl protease K_i determination, cell Aβ_{40} IC_{50} determination and determination of Aβ levels in rat brain and CSF samples were conducted as previously described.[15,16,18]

Synthesis: Unless otherwise mentioned, all the reagents and solvents were obtained from commercial sources and used without further purification. Air sensitive chemistries were performed under an atmosphere of nitrogen or argon. Purification of the final compounds to >95% purity were carried out either using a prepacked silica gel cartridge (Analogix or Biotage or ISCO) or a reverse phase C18 column (mobile phase, A = 0.05% TFA in water and B = 0.05% TFA in acetonitrile, gradient = 10% to 95% B over 10 min). All NMR data unless otherwise specified were collected at 400 MHz on Varian or Bruker instruments. Chemical shifts are reported in ppm relative to the residual solvent peak in the indicated solvent, and for ^{1}H NMR, multiplicities, coupling constants in Hertz, and numbers of protons are indicated parenthetically. Microwave assisted reactions were performed in a Smith synthesizer from Personal Chemistry. Purity and MS information was obtained via LC-electrospray-mass spectroscopy with a C18 column using a gradient of 5% to 95% MeCN in water with 0.05% TFA

as the mobile phase. The purity of the samples was assessed using a UV detector at 254 nm. An additional analytical reverse phase HPLC system was used to assess the purity of final compounds using an ELSD detector and a UV detector monitoring both 220 nm and 254 nm.

***tert*-Butyl ((4aR,7aR)-7a-(5-cyanothiophen-2-yl)-3-methyl-4-oxohexahydro-1H-pyrrolo[3,4-d]pyrimidin-2(3H)-ylidene)carbamate (29)**. To a solution of **26** (1.8 g, 3.1 mmol) in methanol (40 mL) was added 10% palladium on carbon (0.9 g), and the resulting mixture was stirred under the atmospheric of H_2 for 1.5 h. The reaction mixture was filtered, the filtrate was concentrated and the residue was purified using 0 to 100% ethyl acetate in hexanes to provide **27** (1.41 g, 92%). ^{1}H NMR (400 MHz, $CDCl_3$) δ 10.4 (m, 1H), 7.31 (m, 1H), 6.97-6.99 (m, 2H), 4.20 (m, 2H), 3.68-4.06 (m, 4H), 3.50 (m, 1H), 3.30 (s, 3H), 1.53 (s, 9H), 1.01 (m, 2H), 0.03 (s, 9H).

To a solution of **27** (1.41 g, 2.8 mmol) in DMF (15 mL) was added NBS (0.6 g, 3.4 mmol), and the resulting mixture was stirred for 12 h. The reaction mixture was diluted with ethyl acetate (100 mL), washed with brine, and then with water. The organic layer was dried with Na_2SO_4 and concentrated. The crude product was purified by silica gel chromatography using 0 to 100% ethyl acetate in hexanes to provide **28** (0.96 g, 60%). ^{1}H NMR (400 MHz, $CDCl_3$) δ 10.39 (m, 1H), 6.94 (d, J = 4.0 Hz, 1H), 6.76 (m, 1H), 4.20 (m, 2H), 3.68-4.04 (m, 4H), 3.43 (m, 1H), 3.29 (s, 3H), 1.53 (s, 9H), 1.01 (m, 2H), 0.03 (s, 9H).

To a solution of **28** (1.0 g, 1.7 mmol) in DMA (3 mL) were added $PdCl_2$(dppf) (0.2 g, 0.17 mmol), $Zn(CN)_2$ (0.2 g, 1.7 mmol) and Zn powder (0.1 g, 1.7 mmol). The resulting solution was degassed and heated at 80 °C for 4 h. The reaction mixture was then diluted with ethyl acetate and passed through a silica gel plug. The filtrate was evaporated, and to a solution of the resulting material in dichloromethane (5 mL) was added Et_3N (0.5 mL, 3.5 mmol) and $(Boc)_2O$ (0.572 g, 2.6 mmol). The

resulting solution was stirred at rt for 12 h and then evaporated to dryness. The crude product was purified via silica gel chromatography eluting with 25% ethyl acetate in hexanes to provide a Teoc-protected precursor to cyanothiophene core **29** (0.628 g, 71%). ^{1}H NMR (400 MHz, $CDCl_3$) δ 10.47 (m, 1H), 7.51 (d, *J* = 4.5 Hz, 1H), 7.04 (m, 1H), 4.16-4.20 (m, 2H), 3.71-4.04 (m, 4H), 3.46-3.49 (m, 1H), 3.26 (s, 3H), 1.50 (s, 9H), 0.98 (m, 2H), 0.01 (s, 9H). To a solution of this intermediate (1.0 g, 1.9 mmol) in THF (2 mL) was added a solution of 1M TBAF in THF (5.7 mL, 5.7 mmol) at 0 °C, and the resulting solution was warmed to rt over period of 30 minutes and then stirred for additional 3 h. The reaction mixture was evaporated to dryness, and was directly loaded into silica gel column and purified using 100% ethyl acetate to provide **29** (0.56 g, 80%).

General Procedure A for *N*-arylation and Subsequent Boc Removal. To a solution of the pyrrolidine intermediate (1 equiv.) and heteroaryl halide (1.2 equiv.) in toluene (5 mL/mmol of pyrroldine) were added tris(dibenzylidene-acetone)dipalladium(0) (0.1 equiv.), (2-biphenylyl)di-*tert*-butylphosphine (JohnPhos, 0.15 equiv.) and Na-O*t*Bu (2.2 equiv.). The resulting solution was degassed and heated at 70 °C for 3 h, then cooled to room temperature, filtered through a pad of Celite, and the crude material was purified via silica gel chromatography using ethyl acetate in hexanes as the eluant to give an N-arylated product. The Boc protecting group was removed through treament of this material with 20% TFA/CH_2Cl_2 (2.5 mL/mmol). The deprotected compounds were purified by reverse phase HPLC (C18) using 0 to 90% water / acetonitrile with 0.05% TFA.

5-((4aR,7aR)-6-(5-Fluoro-4-methoxypyrimidin-2-yl)-2-imino-3-methyl-4-oxooctahydro-1H-pyrrolo[3,4-d]pyrimidin-7a-yl)thiophene-2-carbonitrile (10). Compound **10** was prepared from compound **29** (38 mg, 0.101 mmol) and 2-chloro-5-fluoro-4-methoxypyrimidine following general

procedure A (2.2 mg, 5%). ^{1}H NMR (400 MHz, CD_3OD) δ 8.05 (d, *J* = 3.3 Hz, 1H), 7.76 (d, *J* = 4.0 Hz, 1H), 7.33 (d, *J* = 4.0 Hz, 1H), 4.41 (d, *J* = 12.4 Hz, 1H), 4.10 (m, 4H), 4.02 (s, 3H), 3.33 (s, 3H). *m/z*: 402.2.

5-((4aR,7aR)-6-(5-Fluoro-4-methoxy-6-methylpyrimidin-2-yl)-2-imino-3-methyl-4-oxooctahydro-1H-pyrrolo[3,4-d]pyrimidin-7a-yl)thiophene-2-carbonitrile (11). Compound **11** was prepared from compound **29** (40 mg, 0.107 mmol) and 2-chloro-5-fluoro-4-methoxy-6-methylpyrimidine following general procedure A (26 mg, 60%). ^{1}H NMR (400 MHz, CD_3OD) δ 7.75 (d, *J* = 4.0 Hz, 1H), 7.32 (d, *J* = 4.0 Hz, 1H), 4.88 (s, 3H), 4.40 (d, *J* = 12.9 Hz, 1H), 4.08 (m, 4H), 3.98 (s, 3H), 3.33 (s, 3H), 2.28 (d, *J* = 2.9 Hz, 3H). *m/z*: 416.2.

***tert*-Butyl ((4aR,7aR)-7a-(5-chlorothiophen-2-yl)-3-methyl-4-oxohexahydro-1H-pyrrolo[3,4-d]pyrimidin-2(3H)-ylidene)carbamate (31)**. To a solution of **27** (1.0 g, 2 mmol) in DMF (15 mL) was added NCS (0.265 g, 4 mmol), and the resulting mixture was stirred at 50 °C for 2 h, and then cooled to room temperature. The reaction mixture was diluted with water and extracted with ethyl acetate (3x50 mL). The organic layer was dried with Na_2SO_4, concentrated and the residue was purified using 25% ethyl acetate in hexanes to provide 5-chlorothiophene **30** (0.846 g, 80%). ^{1}H NMR (400 MHz, $CDCl_3$) δ 10.39 (m, 1H), 6.78 (m, 2H), 4.19-4.21 (m, 2H), 3.71-4.04 (m, 4H), 3.43 (m, 1H), 3.29 (s, 3H), 1.52 (s, 9H), 1.0 (m, 2H), 0.03 (s, 9H).

To a solution of **30** (0.846 g, 1.6 mmol) in THF (2 mL) was added a solution of 1M TBAF in THF (4.8 mL, 2.4 mmol) at 0 °C, and the resulting solution was warmed to rt over period of 30 minutes and then stirred for additional 3 h. The reaction mixture was evaporated to dryness, and was loaded onto silica gel column and purified using 100% ethyl acetate to provide **31** (0.417 g, 75%).

(4aR,7aR)-7a-(5-Chlorothiophen-2-yl)-6-(5-fluoro-4-methoxy-6-methylpyrimidin-2-yl)-2-imino-3-methylhexahydro-1H-pyrrolo[3,4-d]pyrimidin-4(4aH)-one (12). Compound **12** was prepared from compound **31** (20 mg, 0.052 mmol) and 2-chloro-5-fluoro-4-methoxy-6-methylpyrimidine following general procedure A (10 mg, 48%). ^{1}H NMR (400 MHz, CD_3OD) δ 7.03 (d, *J* = 3.9 Hz, 1H), 6.97 (d, *J* = 3.9 Hz, 1H), 4.36 (d, *J* = 12.3 Hz, 1H), 4.07 (m, 4H), 3.98 (s, 3H), 3.33 (s, 3H), 2.29 (d, *J* = 3.0 Hz, 3H). *m/z*: 425.2.

(4aR,7aR)-7a-(5-Chlorothiophen-2-yl)-6-(4-ethyl-5-fluoro-6-methoxypyrimidin-2-yl)-2-imino-3-methylhexahydro-1H-pyrrolo[3,4-d]pyrimidin-4(4aH)-one (13). Compound **13** was prepared from compound **31** (20 mg, 0.052 mmol) 2-chloro-4-ethyl-5-fluoro-6-methoxypyrimidine following general procedure A (10 mg, 46%). ^{1}H NMR (400 MHz, CD_3OD) δ 7.03 (d, *J* = 3.9 Hz, 1H), 6.97 (d, *J* = 3.9 Hz), 4.34 (d, *J*= 12.4 Hz, 1H), 4.08 (m, 4H), 3.98 (s, 3H), 3.33 (s, 3H), 2.65 (qq, *J* = 2.5 Hz, 7.6 Hz, 2H), 1.22 (t, *J* = 7.5 Hz, 3H). *m/z*: 439.2.

(4aR,7aR)-7a-(5-Chlorothiophen-2-yl)-6-(5-fluoro-4-methoxy-6-propylpyrimidin-2-yl)-2-imino-3-methylhexahydro-1H-pyrrolo[3,4-d]pyrimidin-4(4aH)-one (14). Compound **14** was prepared from compound **31** (20 mg, 0.052 mmol) and 2-chloro-5-fluoro-4-methoxy-6-propylpyrimidine following general procedure A (11 mg, 48%). ^{1}H NMR (CD_3OD) δ 7.03 (d, *J* = 4.0 Hz, 1H), 6.97 (d, *J* = 3.9 Hz, 1H), 4.36 (d, *J* = 12.2 Hz, 1H), 4.22 – 4.07 (m, 1H), 4.07 – 4.00 (m, 2H), 3.99 (s, 3H), 3.32 (s, 3H), 2.67 – 2.54 (m, 2H), 1.70 (h, *J* = 7.4 Hz, 2H), 0.95 (t, *J* = 7.4 Hz, 3H). *m/z*: 453.2.

5-((4aR,7aR)-6-(4-Ethoxy-5-fluoro-6-methylpyrimidin-2-yl)-2-imino-3-methyl-4-oxooctahydro-1H-pyrrolo[3,4-d]pyrimidin-7a-yl)thiophene-2-carbonitrile (15). Compound **15** was prepared from compound **29** (60 mg, 0.16 mmol) and 2-chloro-4-ethoxy-5-fluoro-6-methylpyrimidine following general procedure A (14 mg, 20%). ^{1}H NMR (400 MHz, CD_3OD) δ 7.75 (d, *J* = 4.0 Hz, 1H), 7.32 (d, *J* = 4.0 Hz, 1H), 4.48 – 4.42 (q, *J* = 7.1 Hz, 2H), 4.40 (d, *J* = 12.3 Hz, 1H), 4.15 (dd, *J* = 8.7, 7.0 Hz, 1H), 4.11 – 3.98 (m, 4H), 3.32 (s , 3H), 2.28 (d, *J* = 3.0 Hz, 3H), 1.39 (t, *J* = 7.1, 3H). *m/z*: 430.2.

5-((4aR,7aR)-6-(5-Fluoro-4-methyl-6-(methylthio)pyrimidin-2-yl)-2-imino-3-methyl-4-oxooctahydro-1H-pyrrolo[3,4-d]pyrimidin-7a-yl)thiophene-2-carbonitrile (16). To a solution of compound **29** (90 mg, 0.240 mmol) in toluene (3 mL) was added tris(dibenzylidene-acetone)dipalladium (0) (0.026 mmol. 27 mg), 2-cyclohexylphosphino-2'-(*N*,*N*-dimethylamino)biphenyl (0.068 mmol, 24 mg) and sodium *tert*-butoxide (0.77 mmol, 74 mg) and the vial was degassed with nitrogen (evacuate /flush, 3x) and 2-chloro-5-fluoro-4-methyl-6-(methylthio)pyrimidine (0.33 mmol, 63 mg) was added as a solution in toluene (0.2 mL). The reaction mixture was heated at 60 °C for 16 h, then cooled to room temperature, filtered through a pad of Celite, and concentrated. The crude material was purified by flash chromatography using 0% to 60% ethyl acetate in hexanes to afford an *N*-arylated product that was treated with 20% TFA/CH_2Cl_2 (2 mL) to remove the Boc-protecting group. This material was purified by reverse phase HPLC (C18, 35 mL/mim, 10% to 95% MeCN/H_2O, 0.05% TFA) to provide compound **16** (46 mg, 45%). ^{1}H NMR (400 MHz, CD_3OD) δ 7.77 - 7.72 (m, *J* = 3.3 Hz, 1 H), 7.33 (d, *J* = 4.0 Hz, 1 H), 4.53 - 4.42 (m, 1 H), 4.25 - 4.14 (m, 1 H), 4.14 - 4.01 (m, 3 H), 3.33 (s, 3 H), 2.53 (s, 3 H), 2.29 (d, *J* = 2.2 Hz, 3 H).

5-((4aR,7aR)-6-(5-Fluoro-4-methyl-6-(methylamino)pyrimidin-2-yl)-2-imino-3-methyl-4-oxooctahydro-1H-pyrrolo[3,4-d]pyrimidin-7a-yl)thiophene-2-carbonitrile (17). Compound **17** was prepared from compound **29** (53 mg, 0.14 mmol) and *tert*-butyl (2-chloro-5-fluoro-6-methylpyrimidin-4-yl)(methyl)carbamate following general procedure A (21 mg, 38%, yield). ^{1}H NMR (400MHz , CD_3OD) δ 7.76 (d, *J* = 3.9 Hz, 1H), 7.35 (d, *J* = 4.0 Hz, 1H), 4.27 - 4.08 (m, 3H), 3.31 (s, 3H), 3.03 (s, 3H), 2.33 (d, *J* = 3.1 Hz, 3H). *m/z*: 415.2.

(4aR,7aS)-7a-(2,4-difluorophenyl)-6-(5-fluoro-4-methoxy-6-methylpyrimidin-2-yl)-2-imino-3-methyloctahydro-4H-pyrrolo[3,4-d]pyrimidin-4-one (9). To a solution of 2-(2,4-difluorophenyl)acetonitrile **32** (75 g, 0.49 mol) in MeOH (3 L) was added glyoxylic acid (50 % (w/w) in water, 81.8 mL, 0.735 mol). The resulting reaction mixture was cooled to 0 °C and then was added K_2CO_3 (169 g, 1.2 mol) in several portions. After the addition of K_2CO_3, the reaction mixture was heated at 70 °C for 12 h, and then was allowed to cool to room temperature. The resulting white precipitate was collected by filtration and washed with cold water and with methanol to afford **33** as a white solid after drying in a vacuum oven (91 g, 89%). ^{1}H NMR (400 MHz, DMSO-d_6) δ 7.51 (m, 1H), 7.34 (m, 1H), 7.15 (m, 1H), 6.84 (s, 1H).

To a mixture of concentrated sulfuric acid (0.630 L) and 99% formic acid (8.36 L) at rt was added **33** (1424 g, 5.76 mol) in several portions over 15 min. The resulting solution was heated at 110 °C for 3 h and allowed to cool to rt over 12 h. The precipitated solid was collected by vacuum filtration and re-dissolved in toluene (1.5 L). The resulting solution was concentrated under reduced pressure to provide **34** (568 g, 47%) as a white solid. The filtrate from the reaction was then extracted with toluene (3 x 4 L) and the combined extracts concentrated under reduced pressure to afford additional **34** (569 g,

47%) as a white solid. ^{1}H NMR (400 MHz, $CDCl_3$) δ 8.43 (m, 1H), 7.21 (d, 1H), 7.08 (m, 1H), 7.02 (m, 1H).

A solution of **34** (252 g, 1.20 mol) in THF (800 mL) was cooled to 0-5 °C and trifluoroacetic acid (20 mL, 0.260 mol) was then added. To the resulting mixture was added a solution of *N*-(methoxymethyl)-N-(trimethylsilylmethyl)benzylamine **35** (80% pure, 455 g, 1.50 mol) in THF (300 mL) dropwise over 2 h. The internal temperature was monitored and kept below 15 °C. Upon completion of the addition, the cold bath was removed and the reaction mixture was allowed to warm to rt and stirred for 18 h and then the solvents were removed under reduced pressure. Methanol (1.1 L) was added and the reaction mixture was stirred for 12 h. The precipitated solid was collected by vacuum filtration, washed with methanol (400 mL) followed by with diethyl ether (500 mL) and dried to give **36** (257 g, 57%) as an off-white solid. ^{1}H NMR (400 MHz, DMSO-d_6) δ 7.63 (m, 1H), 7.30-7.06 (m, 7H), 3.73 (m, 3H), 3.54 (s, 3H), 3.31 (m, 1H), 3.09 (m, 2H), 2.97 (m, 1H). *m/z*: 376.1.

To a slurry of **36** (250 g, 0.666 mol) in anhydrous toluene (2.22 L) was added triethylamine (67.4 g, 0.666 mol). The resulting suspension was stirred at rt for 10 min, then was added DPPA (202 g, 0.733 mol). The reaction mixture was heated at 66 °C for 30 min and then was cooled to 40-50 °C, and to this mixture was added acetic acid (40.0 g, 0.666 mol) followed by 2-(trimethylsilyl)ethanol (118 g, 0.998 mol). The resulting mixture was heated to gentle reflux for 12 h. The reaction mixture was cooled to room temperature, concentrated under reduced pressure, diluted with ethyl acetate (1 L) and the suspension was washed with saturated aqueous sodium bicarbonate (2 x 800 mL). The organic layer was washed with brine (600 mL), dried over anhydrous sodium sulfate, filtered, and concentrated under reduced pressure. The resulting residue was purified by flash column chromatography (silica gel, 15% EtOAc/heptane) to afford a Teoc protected Curtius product (155 g, 48%) as a light yellow oil. ^{1}H NMR

(400 MHz, $CDCl_3$) δ 7.56 (m, 1H), 7.32 (m, 5H), 6.82 (m, 3H), 4.08 (m, 2H), 3.76 (d, 2H), 3.71 (s, 3H), 3.61 (m, 1H), 3.40 (m, 1H), 3.36 (m, 1H), 3.01 (m, 2H), 0.98 (m, 1H), 0.02 (s, 9H). *m/z*: 491.1.

A solution of HCI (4M in 1,4-dioxane, 313 mL, 1.25 mol) was added to the above material (68.0 g, 0.139 mol). The resulting solution was stirred at rt for 12 h. After this time, the reaction mixture was concentrated under reduced pressure to a syrup and then basified to pH 9 by slow addition of saturated aqueous sodium carbonate. The resulting suspension was extracted with ethyl acetate (4 x 300 mL). The combined extracts were dried over anhydrous sodium sulfate, filtered, and concentrated under reduced pressure. The residue was further dried under high vacuum for 30 min to give amine **37** as a crude mixture that was used directly in the next step. ^{1}H NMR (400 MHz, $CDCl_3$) δ 7.31 (m, 1H), 7.43 (m, 5H), 7.90 (m, 2H), 6.19 (m, 1 H), 4.43 (m, 2H), 4.17 (m, 2H), 4.00 (m, 2H), 3.71 (s, 3H). To a solution of this crude amine **37** in anhydrous DMF (700 mL) was added DIEA (97.0 mL, 0.556 mol), *t*-butyl *N*-[(methylamino)thioxomethyl]carbamate[18] (33.6 g, 0.177 mol) and EDCI (42.4 g, 0.221 mol). The resulting mixture stirred at 30 °C for 24 h. After this time, the reaction mixture was cooled to rt, diluted with ethyl acetate (1.5 L) and washed sequentially with water (4 x 800 mL) and brine (500 mL). The organic layer was dried over anhydrous sodium sulfate, filtered, and concentrated under reduced pressure. The residue was purified by flash column chromatography (silica gel, 15% ethyl acetate/heptane) to afford racemic **38** as a white solid (41.1 g, 63%). The enantiomers were separated using chiral HPLC (Chiralpak AD column, 20 μm, 5 cm x 50 cm, 40 mL/min, 95% hexane/isopropanol) to afford desired enantiomer **39** (slower eluting, t_R = 65 min) and undesired enantiomer **40** (faster eluting, t_R = 34 min). ^{1}H NMR (400 MHz, $CDCl_3$) δ 7.39 (m, 5H), 7.31 (m, 1H), 6.99 (m, 2H), 3.86 (s, 2H), 3.79 (m, 1H), 3.38 (s, 3H), 3.36 (m, 3H), 3.20 (m, 1H), 1.63 (s, 9H). *m/z*: 471.1.

To a solution of **39** (3.57 g, 7.44 mmol) in methanol (30 mL) was added 20% $Pd(OH)_2$ on carbon (0.97 g), and the resulting mixture was stirred under an atmosphere of H_2 at rt for 12 h and then filtered

through Celite. The Celite was washed with MeOH and the combined filtrate and washings were evaporated to give **41** (2.63 g, 91%) which was used without further purification. ^{1} H NMR (400 MHz, $CDCl_3$) δ 7.30 (m, 1H), 7.00 (m, 2H), 4.03 (m, 1 H), 3.91 (m, 2H), 3.72 (m, 1H), 3.58 (m, 1H), 3.35 (s, 3H), δ 1.60 (s, 9H). *m/z*: 381.2.

To a flame-dried and N_2 purged flask was added 2-chloro-5-fluoro-4-methoxy-6-methylpyrimidine (765 mg, 4.33 mmol), 2'-(di-*tert*-butylphosphino)-N,N-dimethylbiphenyl-2-amine (63 mg, 0.18 mmol), $Pd(OAc)_2$ (37 mg, 0.167 mmol) and sodium *tert*-butoxide (705 mg, 7.33 mmol) in one portion. To this mixture was then added a solution of **41** (1.27 g, 3.33 mmol) in anhydrous toluene (10 mL). The reaction mixture was heated at 100 ºC in an oil bath with stirring for 30 min then cooled to rt. The reaction mixture was diluted with CH_2Cl_2 (100 mL) and acidified with 5% aqueous citric acid. The aqueous layer was extracted with CH_2Cl_2 (50 mL). The combined organic layers were washed with saturated aqueous $NaHCO_3$ and brine, dried over $MgSO_4$, filtered and concentrated. The crude mixture was purified by silica gel chromatography (gradient from 0% to 15% EtOAc/hexanes) to afford the corresponding *N*-arylated product (1.29 g, 75% yield). This material was stirred with 20% TFA/DCM (10 mL) at rt for 4 h and then concentrated. The residue was purified by reverse phase HPLC (Novapak HR-C18, 25 mm x 100 mm, 6 µm) gradient from 10% to 90% MeCN/H_2O with 0.1% HCOOH, 35 mL/min) to give **9** (0.56 g, 78%). ^{1}H NMR (400 MHz, CD_3OD) δ 7.40 (m, 1H), 7.18 (m, 1H), 7.07 (m, 1H), 4.55 (dd, *J* = 3.2 Hz, 12.5 Hz, 1H,), 4.21 (m, 2H), 3.98 (s, 1H), 3.29 (s, 3H), 2.29 (d, *J* = 2.9 Hz, 3H). *m/z*: 421.1.

(4aR,7aS)-6-(5-Fluoro-4-methoxy-6-methylpyrimidin-2-yl)-2-imino-3-methyl-7a-phenylhexahydro-1H-pyrrolo[3,4-d]pyrimidin-4(4aH)-one (18). Compound **18** was prepared from 3-phenylfuran-2,5-dione according to the procedures for compound **9** beginning from the [3+2]

cycloaddition step with **35** and using general procedure A for the *N*-arylation and final deprotection. ^{1}H NMR (400 MHz, CD_3OD) δ 7.51 – 7.38 (m, 5H), 4.32 (d, *J* = 12.2 Hz, 1H), 4.17 (dd, *J* = 10.4, 8.7 Hz, 1H), 4.07 (t, *J* = 8.4 Hz, 1H), 3.97 (m, 5H), 3.27 (s, 3H), 2.28 (d, *J* = 2.9 Hz, 3H). *m/z*: 385.2

(4aR,7aS)-6-(5-Fluoro-4-methoxy-6-methylpyrimidin-2-yl)-7a-(2-fluorophenyl)-2-imino-3-methylhexahydro-1H-pyrrolo[3,4-d]pyrimidin-4(4aH)-one (19). Compound **19** was prepared from 2-(2-fluorophenyl)acetonitrile according to the procedures for compound **9** and using general procedure A for the *N*-arylation and final deprotection. ^{1}H NMR (400 MHz, CD_3OD) δ 7.17 - 7.04 (m, 4H), 4.48 (dd, *J* = 2.0 Hz, 12.4 Hz, 1H), 4.33 (dd, *J* = 10.0 Hz, 10.5 Hz, 1H), 4.09 (t, *J* = 9.3 Hz, 1H), 4.02 (d, *J* = 12.4 Hz, 1H), 3.96 (s, 3H), 3.81 (t, *J* = 10.4 Hz, 1H), 3.36 (s, 3 H), 2.29 (d, *J* = 2.9 Hz, 3H). *m/z*: 403.2.

(4aR,7aS)-6-(5-Fluoro-4-methoxy-6-methylpyrimidin-2-yl)-7a-(4-fluorophenyl)-2-imino-3-methylhexahydro-1H-pyrrolo[3,4-d]pyrimidin-4(4aH)-one (20). Compound **20** was prepared from 3-(4-fluorophenyl)furan-2,5-dione according to the procedures for compound **9** beginning from the [3+2] cycloaddition step with **35** and using general procedure A for the *N*-arylation and final deprotection. ^{1}H NMR (400 MHz, CD_3OD) δ 7.56 – 7.48 (m, 2H), 7.25 – 7.18 (m, 2H), 4.32 (d, *J* = 12.3 Hz, 1H), 4.14 (dd, *J* = 9.9, 8.3 Hz, 1H), 4.10 – 4.03 (m, 1H), 4.02 – 3.94 (m, 5H), 3.29 (s, 3H), 2.28 (d, *J* = 3.0 Hz, 3H). *m/z*: 403.2.

(4aR,7aS)-7a-(2,5-Difluorophenyl)-6-(5-fluoro-4-methoxy-6-methylpyrimidin-2-yl)-2-imino-3-methylhexahydro-1H-pyrrolo[3,4-d]pyrimidin-4(4aH)-one (21). Compound **21** was prepared from 2-(2,5-difluorophenyl)acetonitrile according to the procedures for compound **9** and using general procedure A for the *N*-arylation and final deprotection. ^{1}H NMR (400 MHz, CD_3OD) δ 7.37 – 7.21 (m,

2H), 7.14 (m, 1H), 4.54 (dd, *J* = 12.3, 3.1 Hz, 1H), 4.31 – 4.16 (m, 2H), 4.02 – 3.90 (m, 5H), 3.30 (s, 3H), 2.30 – 2.28 (m, 3H). *m/z*: 421.2.

(4aR,7aS)-6-(5-Fluoro-4-methoxy-6-methylpyrimidin-2-yl)-2-imino-3-methyl-7a-(2,4,5-trifluorophenyl)hexahydro-1H-pyrrolo[3,4-d]pyrimidin-4(4aH)-one (22). Compound **22** was prepared from 2-(2,4,5-trifluorophenyl)acetonitrile according to the procedures for compound **9** and using general procedure A for the *N*-arylation and final deprotection. ^{1}H NMR (400 MHz, CD_3OD) δ 7.37 - 7.17 (m, 2H), 4.24 (d, *J* = 11.4 Hz, 1H), 4.14 (t, *J* = 9.7 Hz, 1H), 3.96 (s, 3H), 4.00 - 3.84 (m, 2H), 3.78 - 3.66 (m, 1H), 3.22 (s, 3H), 2.27 (s, 3H). *m/z*: 439.2.

(4aR,7aS)-7a-(2,6-Difluorophenyl)-6-(5-fluoro-4-methoxy-6-methylpyrimidin-2-yl)-2-imino-3-methylhexahydro-1H-pyrrolo[3,4-d]pyrimidin-4(4aH)-one (23). A flask was charged sequentially with diethylacetylene dicarboxylate **42** (5.0 g, 29 mmol), 2,6-difluorophenylboronic acid **43** (5.57 g, 35.3 mmol), 1,4-dioxane (90 mL), tetrakis(triphenylphosphine)palladium(0) (1.36 g, 1.18 mmol), and acetic acid (0.167 mL, 2.94 mmol). The resulting mixture was degassed by evacuation and back-filled with N_2 (3X) and was then immersed in an 80 °C oil bath. After 16 h, the reaction was diluted with water and extracted twice with EtOAc. The combined organic portions were washed with sat. aq. $NaHCO_3$ and brine, dried over $MgSO_4$, filtered and concentrated. The crude sample was subjected to column chromatography (330 g silica, 90 mL/min, 0% to 35% EtOAc/hexanes) to give diethyl 2-(2,6-difluorophenyl)maleate (2.85 g, 34%). ^{1}H NMR (400 MHz, $CDCl_3$) δ 7.32 (m, 1H) 6.94 (m, 2H), 6.45 (s, 1H), 4.30 (t, *J* = 12.2 Hz, 2H) overlapping 4.26 (t, *J* = 12.2 Hz, 2H), 1.32 (q, *J* = 12.2 Hz, 3H) overlapping 1.30 (q, *J* = 12.2 Hz, 3H).

To a solution of diethyl 2-(2,6-difluorophenyl)maleate (1.34 g, 4.71 mmol) in mixture of THF

(100 mL) and water (35 mL) was added lithium hydroxide monohydrate (0.99 g, 34 mmol). The resulting mixture was immersed in a 40 °C oil bath and stirred vigorously. After 18 h at 40 °C, the reaction was cooled, diluted with 1N HCl and was extracted twice with THF/EtOAc (1/3). The combined organic portions were washed with brine, dried over $MgSO_4$, filtered and concentrated. This material was dissolved in acetic anhydride (35 mL, 260 mmol) and immersed in a 90 °C oil bath. After 90 min, the mixture was concentrated to a semisolid and dried azeotropically with toluene (50 mL) to give 3-(2,6-difluorophenyl)furan-2,5-dione **44.** ^{1}H NMR (400 MHz, $CDCl_3$) δ 7.53 (m, 1H), 7.09 (m, 3H).

To a solution of **44** (46.8 g, 180 mmol) in THF (400 mL) was added *N*-benzyl-*N*-methoxymethyl-*N*-(trimethylsilyl)methylamine **35** (64.5 mL, 352 mmol) and then trifluoroacetic acid (1.39 mL, 18.0 mmol) at 0 °C. The cooling bath was removed and the mixture was allowed to stir at rt. After 75 min, the reaction mixture was immersed in a bath at -60 °C, and a premixed solution of triethylamine (50.2 mL, 360 mmol) in methanol (180 mL) was added *via* dropping funnel over 15 min. The resulting mixture was allowed to warm to rt and stirred for 2.5 days. The precipitated solid was collected via filtration and the filtrate was partially concentrated causing additional solid to precipitate that was isolated by filtration. A third batch of solid was obtained by filtration after the mother liquor was allowed to stand for one week. The combined yield for the three crops of **45** was 48.4 g (56% as the triethylammonium salt). A portion of this material was converted to its HCl salt by treatment with 4N HCl/dioxane. *m/e* = 376.

To a solution of compound **45** (8.5 g, 18 mmol) in MeOH (350mL) was added 4N HCl in dioxane (100 mL) and then concentrated. The resulting residue was then redissolved in MeOH (350 mL) and 20% palladium hydroxide on carbon (4.0 g) was added in two batches. The mixture was stirred vigorously, and the flask was evacuated and back-filled with H_2 from a balloon (3X). The reaction was

then kept under the atmosphere of H_2 for 3 h. At that time, the flask was evacuated and back-filled with N_2 (2X), and the mixture was filtered through a Celite pad with copious MeOH washes. The filtrate was concentrated to give a crude product that was dissolved in THF (200 mL) and treated with triethylamine (6.2 mL, 44 mmol). Dioxane (100 mL) was added, followed by benzyl chloroformate (3.0 mL, 21 mmol). After 1 h, the reaction was diluted with 1N HCl and was extracted with 1:1 THF:EtOAc (3X). The organic portions were combined, washed with brine, dried over $MgSO_4$, filtered, and concentrated. The crude sample was taken up in toluene (100 mL), reconcentrated, and subjected to column chromatography (330 g silica, 80 mL/min, 0% to 10% MeOH/DCM) to give **46** (4.8 g, 64%). ^{1}H NMR (400 MHz, $CDCl_3$) δ 7.34 (m, 4H), 7.31 (m, 2H), 6.89 (m, 2H), 5.15 (dq, J_q = 12.0 Hz, J_d = 4.0 Hz, 2H), 4.63-4.51 (m, 1H), 3.98 (m, 2H), 3.86 (m, 1H), 3.77 (dd, J = 16.0, 2.8 Hz, 1H), 3.71 (m, 3H).

A round bottomed flask was charged with **46** (4.8 g, 11 mmol), toluene (35 mL), triethyl amine (3.19 mL, 22.9 mmol) and DPPA (3.21 mL, 14.9 mmol). The mixture was immersed in a 75 °C oil bath. After 3 h at 75 °C, 2-(trimethylsilyl)ethanol (6.56 mL, 45.8 mmol) was added and the resulting mixture was heated at 110 °C for 2 h. Then the reaction mixture was cooled to rt and concentrated. The crude sample was subjected to column chromatography (330 g silica, 100 mL/min, 0% to 50% EtOAc/hexanes) to give a Teoc protected amine (4.1 g, 67%). This material was mixed with 4.0 M of HCl in dioxane (38 mL) and allowed to stir at rt for 20 h. The reaction mixture was concentrated to viscous gum to provide **47**, which was taken to next step without further purification. *m/e* = 391.

To a mixture of **47** (3.5 g, 8.2 mmol) and DMF (40 mL) was added DIEA (5.71 mL, 32.8 mmol), *t*-butyl *N*-[(methylamino)thioxomethyl]carbamate[18] (1.95 g, 10.3 mmol) and EDCI (2.36 g, 12.3 mmol). The resulting mixture stirred at room temperature for 6.5 days. At that time, the reaction mixture was diluted with water and EtOAc and stirred vigorously until both phases cleared. The phases were seaprated, and the aqueous layer was extracted with EtOAc (2x). The combined organic layers were

washed with saturated aqueous $NaHCO_3$ (3x) and brine, dried over MgSO4, filtered and concentrated to a light brown oil. This crude sample was subjected to column chromatography (120 g silica, 0-40% EtOAc/hexanes, 60 mL/min,) to give **48** (2.4 g, 57%). The enantiomers of **48** were separated by chiral HPLC (AD column, 15% i-PrOH / hexanes, 80 mL/min) to give undesired enantiomer **49** (faster eluting, t_R ~ 25 min) and desired enantiomer **50** (slower eluting, t_R ~40 min). ^{1}H NMR for **50**: (400 MHz, $CDCl_3$) δ 10.57 – 10.48 (m, 1H), 7.42 – 7.26 (m, 6H), 6.95 (tq, *J* = 8.3, 2.8, 2.4 Hz, 2H), 5.24 – 5.14 (m, 1H), 5.17 – 5.06 (m, 1H), 4.57 (dt, *J* = 12.3, 3.0 Hz, 0.5H), 4.46 (dt, *J* = 12.2, 3.0 Hz, 0.5 H), 4.20 – 3.94 (m, 2H), 3.76 (dd, *J* = 12.3, 6.5 Hz, 1H), 3.63 (td, *J* = 10.3, 7.5 Hz, 1H), 3.27 (d, *J* = 6.0 Hz, 3H), 1.50 (d, *J* = 1.8 Hz, 10H).

Compound **50** (1.2 g, 2.3 mmol) was dissolved in MeOH (15 mL) and 20% palladium hydroxide on carbon (1:4, palladium hydroxide: carbon black, 0.5 g) was added. The mixture was evacuated and back filled with H_2 from a balloon (5x) and then allowed to stir under the H_2 atmosphere. After 5 h, the reaction mixture was filtered through a Celite plug. The filtrate was concentrated to give compound **51** that was carried forward without further purification. ^{1}H NMR (400 MHz, $CDCl_3$) δ 10.30 (s, 1H), 7.36 – 7.22 (m, 1H), 6.99 – 6.85 (m, 2H), 3.94 (dt, *J* = 12.8, 3.1 Hz, 1H), 3.76 – 3.67 (m, 1H), 3.70 – 3.51 (m, 1H), 3.29 (s, 3H), 3.40 – 3.22 (m, 2H), 1.51 (s, 9H).

A microwave vial was charged with **51** (180 mg, 0.473 mmol), 2-chloro-5-fluoro-4-methoxy-6-methylpyrimidine (125 mg, 0.708 mmol), 2-(di-*tert*-butylphosphino)biphenyl (21 mg, 0.070 mmol), tris(dibenzylideneacetone)dipalladium(0) (27mg, 0.029 mmol), toluene (2.5 mL) and sodium tert-butoxide (100 mg, 1.041 mmol). The resulting solution was degassed and back filled with nitrogen (3x). The reaction was then sealed and immersed in an oil bath and heated at 65 °C for 4 h. After cooling to rt, the reaction mixture was diluted with water and ethyl acetate and stirred vigorously until both phases cleared. The phases were separated, and the aqueous portion was extracted with ethyl acetate. The

combined organic portions were washed with brine, dried over $MgSO_4$, filtered, and concentrated. The crude product was subjected to column chromatography (40 g silica, 40 mL/min, 0 to 50% ethyl acetate in hexanes) to give the corresponding *N*-arylated product (112 mg, 46%). This material was dissolved in DCM (5 mL) and treated with trifluoroacetic acid (1.5 mL). The resulting mixture was allowed to stand at rt for 3 h and was then concentrated and subjected to reverse phase HPLC (C18, 35 mL/mim, 10% to 95% MeCN/H_2O, 0.1% HCO_2H) to afford compound **23** (83 mg, 63%). ^{1}H NMR (400 MHz, CD_3OD) δ 7.50 (tt, *J* = 8.4, 6.2 Hz, 1H), 7.17 – 7.08 (m, 2H), 4.92 (m, 1H), 4.35 (t, *J* = 9.2 Hz, 1H), 4.26 – 4.15 (m, 1H), 3.99 (s, 3H), 3.95 – 3.82 (m, 2H), 3.30 (s, 3H), 2.29 (d, *J* = 2.9, 3H). *m/z*: 421.2.

1-((Benzyloxy)carbonyl)-4-(methoxycarbonyl)-3-(2,3,6-trifluorophenyl)pyrrolidine-3-carboxylic acid (56). To a solution of 2-(bromomethyl)-1,3,4-trifluorobenzene **52** (68 g, 292 mmol) in ethanol (80 mL) and water (20 mL) was added NaCN (25 g, 526 mmol) and the resulting solution was heated at reflux for 12 h. The reaction mixture was cooled to rt and extracted with ethyl acetate. The organic layer was dried with $MgSO_4$ and purified using 0 to 100% ethyl acetate in hexanes to provide 2-(2,3,6-trifluorophenyl)acetonitrile (44 g, 79% yield). ^{1}H NMR (400 MHz, $CDCl_3$) δ 7.22 – 7.12 (m, 1H), 6.95 – 6.88 (m, 1H), 3.74 (t, *J* = 1.2 Hz, 2H).

To a solution of this 2-(2,3,6-trifluorophenyl)acetonitrile (33 g, 198 mmol) in methanol (200 mL) was added glyoxalic acid monohydrate (27 g, 297 mmol), and the resulting mixture was cooled to 0 °C. Solid K_2CO_3 (68 g, 495 mmol) was added in several portions while cooling the reaction mixture at 0 °C. The reaction mixture was slowly warmed to rt, then stirred for 4 h. It was filtered, and the filtrate was evaporated to yield a solid mass, which was dissolved carefully in 10% conc. H_2SO_4 in formic acid (500 mL), and was heated at 100 °C for 12 h. The reaction mixture was diluted with water, extracted with ethyl acetate to yield the crude 2-(2,3,6-trifluorophenyl)maleic acid. This di-acid was dissolved in 5%

conc. H_2SO_4 in methanol (500 mL) and heated at reflux for 12 h. The resulting mixture was evaporated to dryness, then it was diluted with water, extracted with ethyl acetate, the organic layer was dried with $MgSO_4$, concentrated and purified using 0 to 100% ethyl acetate in hexanes to provide dimethyl 2-(2,3,6-trifluorophenyl)maleate **53** (21 g, 41%). ^{1}H NMR (600 MHz, $CDCl_3$) δ 7.23 – 7.12 (m, 1H), 6.89 (tddd, *J* = 9.2, 3.8, 2.2, 0.7 Hz, 1H), 6.47 (t, *J* = 0.8 Hz, 1H), 3.83 (t, *J* = 1.2 Hz, 3H), 3.81 (t, *J* = 0.9 Hz, 3H).

To a solution of dimethyl 2-(2,3,6-trifluorophenyl)maleate **53** (20 g, 72 mmol) in THF (200 ml) was added *N*-benzyl-1-methoxy-*N*-((trimethylsilyl)methyl)methanamine **35** (26 g, 109 mmol) at 0 °C followed by catalytic amount of trifluoroacetic acid (0.4 mL, 7.2 mmol). The reaction mixture was slowly warmed to rt and stirred for 4 h. The resulting solution was evaporated to dryness and purified via silica gel chromatography using 0 to 100% ethyl acetate in hexanes to provide dimethyl 1-benzyl-3-(2,3,6-trifluorophenyl)pyrrolidine-3,4-dicarboxylate (29 g, 100%). ^{1}H NMR (600 MHz ,$CDCl_3$) δ 7.35 – 7.19 (m, 6H), 7.06 (qd, *J* = 9.0, 4.8 Hz, 1H), 6.79 (dddd, *J* = 11.4, 9.2, 4.1, 2.3 Hz, 1H), 3.84 – 3.78 (m, 1H), 3.75 (s, 2H), 3.71 (s, 3H), 3.65 (s, 3H), 3.46 – 3.36 (m, 2H), 3.19 (d, *J* = 8.8 Hz, 2H). A solution of this dimethyl 1-benzyl-3-(2,3,6-trifluorophenyl)pyrrolidine-3,4-dicarboxylate (30 g) in 15% H_2SO_4 (300 mL) was heated under reflux for 24 h. The reaction mixture was cooled to room temperature, and the pH of the solution was adjusted to 3 using 6N NaOH. Compound **54** precipitated from this mixture and was collected, dried and taken to the next step.

A solution of this 1-benzyl-3-(2,3,6-trifluorophenyl)pyrrolidine-3,4-dicarboxylic acid **54** (30 g, 79 mmol) in acetic anhydride (100 mL) was heated at 90 °C for 1 h. The resulting mixture was evaporated to dryness to obtain the anhydride, which was dissolved in dichloromethane (200 mL) and treated with a mixture of methanol (30 mL) and triethylamine (16.5 mL) at -78 °C. The resulting

mixture was slowly warmed to rt over 12 h. The reaction mixture was evaporated to dryness and the crude product **55** was taken directly to the next step.

To a solution of the above crude 1-((benzyloxy)carbonyl)-4-(methoxycarbonyl)-3-(2,3,6-trifluorophenyl)pyrrolidine-3-carboxylic acid **55** (assumed to be 79 mmol) in methanol (400 mL) was added $Pd(OH)_2$ (7.5 g, 10% by wt.), and the resulting mixture was stirred under one atmosphere of H_2 for 3 h. The solution was then filtered through a pad of Celite, and the filtrate was evaporated to dryness to obtain the corresponding free amine. To this crude amine in THF (1000 mL) at 0 °C was added benzyl chloroformate (25 mL, 122 mmol) followed by triethylamine (20 mL, 143 mmol). The resulting mixture was warmed to rt over 30 minutes and stirred for 12 h. The reaction mixture was diluted with ethyl acetate and washed with 1N HCl. The organic layer was separated, dried with $MgSO_4$, concentrated and purified via silica gel chromatography using 10% methanol in dichloromethane to provide compound **56** (25 g, 79%) ^{1}H NMR (600 MHz, $CDCl_3$,) δ 7.37 – 7.25 (m, 5H), 7.15 – 7.05 (m, 1H), 6.98 (dddd, *J* = 11.6, 7.6, 3.9, 2.3 Hz, 1H), 5.13 (s, 2H), 4.43 (ddt, *J* = 10.3, 4.9, 2.6 Hz, 1H), 4.12 (dt, *J* = 15.8, 9.2 Hz, 1H), 3.94 – 3.71 (m, 3H), 3.67 (d, *J* = 3.7 Hz, 3H).

(4aR,7aS)-6-(5-Fluoro-4-methoxy-6-methylpyrimidin-2-yl)-2-imino-3-methyl-7a-(2,3,6-trifluorophenyl)hexahydro-1H-pyrrolo[3,4-d]pyrimidin-4(4aH)-one (24). Compound **24** was prepared from compound **56** according to the procedures outlined for compound **23** beginning from the Curtius rearrangement step. ^{1}H NMR (400 MHz, CD_3OD) δ 7.49 - 7.38 (m, 1H), 7.18 - 7.08 (m, 1H), 4.89 - 4.85 (m, 1H), 4.39 (t, *J* = 9.7 Hz, 1H), 4.22 (t, *J* = 10.5 Hz, 1H), 3.98 (s, 3H), 3.96 - 3.85 (m, 2H), 3.28 (s, 3H), 2.28 (d, *J* = 2.9 Hz, 3H). *m/z*: 439.5.

(4aR,7aS)-6-(5-Fluoro-4-methoxy-6-methylpyrimidin-2-yl)-2-imino-3-methyl-7a-(2,3,4,6-tetrafluorophenyl)hexahydro-1H-pyrrolo[3,4-d]pyrimidin-4(4aH)-one (25). Compound **25** was prepared from 2-(bromomethyl)-1,3,4,5-tetrafluorobenzene according to the procedures described for compounds **56** and **24**. ^{1}H NMR (400 MHz, CD_3OD) δ 7.35 - 7.23 (m, 1H), 4.88 - 4.84 (m, 1H), 4.38 (t, *J* = 9.7 Hz, 1H), 4.24 (dd, *J* = 9.8 Hz, 10.7 Hz, 1H), 4.01 (s, 3H), 3.97 - 3.86 (m, 2H), 3.30 (s, 3H), 2.31 (d, *J* = 2.9 Hz, 3H). *m/z*: 457.3.

ASSOCIATED CONTENT

Supporting Information. Synthetic procedures for preparation of the pyrimidine reagents used to make compounds **8**-**25**, the synthesis of compound **8,** procedures for incubation of compound **6** with CYP3A4 in the presence and absence of glutathione, methods for determination of rhesus monkey plasma, CSF and cortical Aβ_{40}, Aβ_{42} and sAPPβ levels and methods for determination of cynomolgus monkey CSF and cortical Aβ_{40} levels. This material is available free of charge via the Internet at http://pubs.acs.org.

Accession Codes. Atomic coordinates for BACE1/inhibitor complexes will be deposited at the Protein Data Bank. Authors will release the atomic coordinates and experimental data upon article publication. PDB codes: **6**, 5hd0; **7**, 4h3g; **8**, 5hdu; **11**, 5hdv; **15**, 5hdx; **16**, 5hdz; **17**, 5he5; **23**, 5he4.

AUTHOR INFORMATION

Corresponding Authors

*To whom correspondence should be addressed:

A. W. S. Telephone: +1 732-594-1960. E-mail: andrew.stamford@merck.com

J. N. C. Telephone: +1 908-740-4049. E-mail: jared.cumming@merck.com

ACKNOWLEDGMENTS

We thank T.-M. Chan for his help in compound characterization and Qin Jiang, Laura M. Rossiter, Sarah K. Zeile and Meagan M. Ryan (Albany Molecular Research Inc.) for their contributions to synthesis. Li-Kang Zhang, Junling Gao, and Charles Ross are thanked for their help in LCMS analysis of the compounds. Use of the IMCA-CAT beamline 17-ID (or 17-BM) at the Advanced Photon Source was supported by the companies of the Industrial Macromolecular Crystallography Association through a contract with Hauptman-Woodward Medical Research Institute. Use of the Advanced Photon Source was supported by the U.S. Department of Energy, Office of Science, Office of Basic Energy Sciences, under Contract No. DE-AC02-06CH11357.

ABBREVIATIONS USED

CatD, cathepsin D; DIEA, diisopropylethylamine; DPPA, diphenylphosphoryl azide; EDCI, 1-ethyl-3-(3-dimethylaminopropyl)carbodiimide hydrochloride; ER, efflux ratio; Gly, glycine; IPA, isopropyl alcohol; K_d, dissociation constant; MDCK, Madin-Darby canine kidney epithelial cell line; MDR1, multidrug resistance protein 1; P_{app}, apparent premeability coefficient; Teoc, 2,2,2-trichloroethoxycarbonyl; Trp, tryptophan; Tyr, tyrosine.

REFERENCES

1. Alzheimer's Association. 2015 Alzheimer's Disease Facts and Figures, http://www.alz.org/facts/downloads/facts_figures_2015.pdf (accessed February 13, 2016).
2. Alzheimer's Disease International. World Alzheimer Report 2015, http://www.alz.co.uk/research/WorldAlzheimerReport2015.pdf (accessed February 13, 2016).

3. (a) Tariot, P. N.; Federoff, H. J. Current treatment for Alzheimer disease and future prospects. *Alzheimer Dis. Assoc. Disord.* **2003**, *17*, S105-S113. (b) Nordberg, A. Mechanisms behind the neuroprotective actions of cholinesterase inhibitors in Alzheimer disease. *Alzheimer Dis. Assoc. Disord*. **2006**, *20*, S12-S18. (c) Bullock, R. Efficacy and safety of memantine in moderate-to-severe Alzheimer disease: the evidence to date. *Alzheimer Dis. Assoc. Disord*. **2006**, *20*, 23-29.

4. (a) Lambert, J-C.; Amouyel, P. Genetics of Alzheimer's disease: new evidences for an old hypothesis? *Curr. Opin. Genet. Dev*. **2011**, *21*, 295-301. (b) Walter, J.; Kaether, C.; Steiner, H.; Haass, C. The cell biology of Alzheimer's disease: uncovering the secrets of secretases. *Curr. Opin. Neurobiol.* **2001**, *11*, 585-590. (c) Stege, G. J. J.; Bosman, G. J. C. G. M. The biochemistry of Alzheimer's disease. *Drugs Aging* **1999**, *14*, 437-446. (d) Mucke, L.; Neuroscience: Alzheimer's disease. *Nature* **2009**, *461*, 895-897.

5. (a) Karran, E.; Mercken, M.; De Strooper, B. The amyloid cascade hypothesis for Alzheimer's disease: an appraisal for the development of therapeutics. *Nat. Rev. Drug Discovery* **2011**, *10*, 698-711. (b) Jonsson, T.; Atwal, J. K.; Steinberg, S.; Snaedal, J.; Jonsson, P.V.; Bjornsson, S.; Stefansson, H.; Sulem, P.; Gudbjartsson, D.; Maloney, J.; Hoyte, K.; Gustafson, A.; Liu, Y.; Lu, Y.; Bhangale, T.; Graham, R. R.; Huttenlocher, J.; Bjornsdottir, G.; Andreassen, O. A.; Joensson, E. G.; Palotie, A.; Behrens, T.W.; Magnusson, O. T.; Kong, A.; Thorsteinsdottir, U.; Watts, R. J.; Stefansson, K. A mutation in APP protects against Alzheimer's disease and age-related cognitive decline. *Nature* **2012**, *488*, 96-99. (c) Hardy, J.; Selkoe, D. J. The Amyloid hypothesis of Alzheimer's disease: Progress and problems on the road to therapeutics. *Science* **2002**, *297*, 353–356. (d) Korczyn, A. D. The amyloid cascade hypothesis. *Alzheimer's Dementia* **2008**, *4*, 176–178. (e) Hardy, J. Has the amyloid cascade hypothesis for Alzheimer's been proved? *Curr. Alzheimer Res*. **2006**, *3*, 71–73. (f) Selkoe, D. Alzheimer's disease: genes, proteins, and therapy.

Physiol. Rev. **2001**, *81*, 741–766. (g) Archer, H. A.; Edison, P.; Brooks, D. J.; Barnes, J.; Frost, C.; Yeatman, T. Amyloid load and cerebral atrophy in Alzheimer's disease: a 11C-BIP positron emission tomography study. *Ann. Neurol*. **2006**, *60*, 145–147.

6. (a) Doody, R. S.; Raman, R.; Farlow, M.; Iwatsubo, T.; Vellas, B.; Joffe, S.; Kieburtz, K.; He, F.; Sun, X.; Thomas, R. G.; Aisen, P. S.; Siemers, E.; Sethuraman, G.; Mohs, R. A Phase 3 trial of semagacestat for treatment of Alzheimer's disease. *N. Engl. J. Med.*, **2013**, *369*, 341-350. (b) DeStrooper, B. Lessons from a failed γ-secretase Alzheimer trial. *Cell*, **2014**, *159*, 721-726.
7. (a) Reardon, S. Alzheimer antibody drugs show questionable potential. *Nat. Rev. Drug Discovery* **2015**, *14*, 591-592. (b) Karran, E.; Hardy, J. A critique of the drug discovery and phase 3 clinical programs targeting the amyloid hypothesis for Alzheimer disease. *Ann. Neurol.* **2014**, *76*, 185-205. (c) Prins, N. D.; Scheltens, P. Treating Alzheimer's disease with monoclonal antibodies: current status and outlook for the future. *Alzheimers Res. Ther*. **2013**, *5*, 56-61.
8. (a) Luo, Y.; Bolon, B.; Kahn, S.; Bennett, B. D.; Babu-Khan, S.; Denis, P.; Fan, W.; Kha, H; Zhang, J.; Gong, Y.; Martin, L.; Louis, J. C.; Yan, Q.; Richards, W. G.; Citron, M; Vassar, R. Mice deficient in BACE1, the Alzheimer's beta secretase, have normal phenotype and abolished beta-amyloid generation. *Nat. Neurosci*. **2001**, *4*, 231−232. (b) Luo, Y.; Bolon, B.; Damore, M. A.; Fitzpatrick, D.; Liu, H.; Zhang, J.; Yan, Q.; Vassar, R.; Citron, M. BACE1 (beta secretase) knockout mice do not acquire compensatory gene expression changes or develop neural lesions over time. *Neurobiol. Dis*. **2003**, *14*, 81−88.
9. McConlogue, L.; Buttini, M.; Anderson, J. P.; Brigham, E. F.; Chen, K. S. Freedman, S. B; Games D.; Johnson-Wood, K.; Lee, M.; Zeller, M.; Liu, W.; Motter, R.; Sinha S. Partial reduction of BACE1 has dramatic effects on Alzheimer plaque and synaptic pathology in APP transgenic mice. *J. Biol. Chem.* **2007**, *282*, 26326-26334.

10. Vassar, R.; Kuhn, P-H.; Haass, Ch.; Kennedy, M. E.; Rajendran, L.; Wong, P. C.; Lichtenthaler, S. F. J. Function, therapeutic potential and cell biology of BACE proteases: current status and future prospects. *J. Neurochem*. **2014**, *130*, 4-28.

11. (a). Willem, M.; Garratt, A. N.; Novak, B.; Citron, M.; Kaufmann, S.; Rittger, A.; DeStrooper, B.; Saftig, P.; Birchmeier, C.; Haass C. Control of peripheral nerve myelination by the β-secretase BACE1. *Science* **2006**, *314*, 664-666. (b) Hu, X.; Hicks, C. W.; He, W.; Wong, P.; Macklin, W. B.; Trapp, B. D.; Yan R. Bace1 modulates myelination in the central and peripheral nervous system. *Nat. Med.* **2006**, *9*, 1520-1525.

12. Cheret, C.; Michael Willem, M. I.; Fricker, F. R.; Wende, H.; Wulf-Goldenberg, A.; Tahirovic, S.; Nave, K.-A.; Saftig, P.; Haass, C.; Garratt, A. N.; Bennett , D. L.; Birchmeier, C. Bace1 and neuregulin-1 cooperate to control formation and maintenance of muscle spindles. *EMBO J.* **2013**, *32*, 2015-2028.

13. Ghosh, A. K.; Osswald, H. L. BACE1 (β-secretase) inhibitors for the treatment of Alzheimer's disease. *Chem. Soc. Rev.* **2014**, *43*, 6765-6813.

14. (a) Iserloh, U.; Wu, Y.; Cumming, J. N.; Pan, J.; Wang, L. Y.; Stamford, A. W.; Kennedy, M. E.; Kuvelkar, R.; Chen, X.; Parker, E. M.; Strickland, C.; Voigt, J. Potent pyrrolidine and piperidine-based BACE-1 inhibitors. *Bioorg. Med. Chem. Lett*. **2008**, *18*, 414 -417. (b) Iserloh, U.; Pan, J.; Stamford, A. W.; Kennedy, M. E.; Zhang, Q.; Zhang, L.; Parker, E. M.; McHugh, N. A.; Favreau, L.; Strickland, C.; Voigt, J. Discovery of an orally efficacious 4-phenoxypyrrolidine-based BACE-1 inhibitor. *Bioorg. Med. Chem. Lett*. **2008**, *18*, 418 – 422. (c) Cumming, J. N.; Le, T. X.; Babu, S.; Carroll, C.; Chen, X.; Favreau, L.; Gaspari, P.; Guo, T.; Hobbs, D. W.; Huang, Y.; Iserloh, U.; Kennedy, M. E.; Kuvelkar, R.; Li, G.; Lowrie, J.; McHugh, N. A.; Ozgur, L.; Pan, J.; Parker, E. M.; Saionz, K.; Stamford, A. W.; Strickland, C.; Tadesse, D.; Voigt, J.; Wang,

L.; Wu, Y.; Zhang, L.; Zhang, Q. Rational design of novel potent piperazinone and imidazolidinone BACE1 inhibitors. *Bioorg. Med. Chem. Lett*. **2008**, *18*, 3236 – 3241. (d) Weiss, M. M.; Williamson, T.; Babu-Khan, S.; Bartberger, M. D.; Brown, J.; Chen, K.; Cheng, Y.; Citron, M.; Croghan, M.D.; Dineen, T. A.; Esmay, J.; Graceffa, R. F.; Harried, S. S.; Hickman, D.; Hitchcock, S. A.; Horne, D. B.; Huang, H.; Imbeah-Ampiah, R.; Judd, T.; Kaller, M.R.; Kreiman, C. R.; La, D. S.; Li, V.; Lopez,P.; Louie, S.; Monenschein, H.; Nguyen, T. T.; Pennington, L. D.; Rattan, C.; San Miguel, T.; Sickmier, E. A.; Wahl, R. C.; Wen, P. H.; Wood, S.; Xue, Q.; Yang, B. H.; Patel, V. F.; Zhong, W. Design and preparation of a potent series of hydroxyethylamine containing β-secretase inhibitors that demonstrate robust reduction of central β-amyloid. *J. Med. Chem*. **2012**, *55*, 9009-9024. (e) Dineen, T. A.; Weiss, M. M.; Williamson, T.; Acton, P.; Babu-Khan, S.; Bartberger, M. D.; Brown, J.; Chen, K.; Cheng, Y.; Citron, M.; Croghan, M. D.; Dunn, R. T.; Esmay, J.; Graceffa, R. F.; Harried, S. S.; Hickman, D.; Hitchcock, S. A.; Horne, D. B.; Huang, H.; Imbeah-Ampiah, R.; Judd, T.; Kaller, M. R.; Kreiman, C. R.; La, D. S.; Li, V.; Lopez, P.; Louie, S.; Monenschein, H.; Nguyen, T. T.; Pennington, L. D.; San Miguel, T.; Sickmier, E. A.; Vargas, H. M.; Wahl, R. C.; Wen, P. H.; Whittington, D. A.; Wood, S.; Xue, Q.; Yang, B. H.; Patel, V.F.; Zhong, W. Design and synthesis of potent, orally efficacious hydroxyethylamine derived β-Site amyloid precursor protein cleaving enzyme (BACE1) inhibitors. *J. Med. Chem*. **2012**, *55*, 9025-9044.

15. Wang, Y.-S.; Strickland, C.; Voigt, J. H.; Kennedy, M. E.; Beyer, B. M.; Senior, M. M.; Smith, E. M.; Nechuta, T. L.; Madison, V. S.; Czarniecki, M.; McKittrick, B. A.; Stamford, A. W.; Parker, E. M.; Hunter, J. C.; Greenlee, W. J.; Wyss, D. F.; Application of fragment-based NMR screening, X-ray crystallography, structure- based design, and focused chemical library design to

identify novel μM leads for the development of nM BACE-1 (β-site APP cleaving enzyme 1) inhibitors. *J. Med. Chem*. **2010**, *53*, 942-950.

16. Zhu, Z.; Sun, Z-Y.; Ye, Y.; Voigt, J.; Strickland, C.; Smith, E. M.; Cumming, J.; Wang, L.; Wong, J.; Wang, Y-S.; Wyss, D. F.; Chen, X.; Kuvelkar, R.; Kennedy, M. E.; Favreau, L.; Parker, E.; McKittrick, B. A.; Stamford, A.; Czarniecki, M.; Greenlee, W.; Hunter, J.C. Discovery of cyclic acylguanidines as highly potent and selective *β*-site amyloid cleaving enzyme (BACE) inhibitors: part I; inhibitor design and validation. *J. Med. Chem*. **2010**, 53, 951–965.
17. Cumming, J. N.; Smith, E. M.; Wang, L.; Misiaszek, J.; Durkin, J.; Pan, J.; Iserloh, U.; Wu, Y.; Zhu, Z.; Strickland, C.; Voigt, J.; Chen, X.; Kennedy, M. E.; Kuvelkar, R.; Hyde, L. A.; Cox, K.; Favreau, L.; Czarniecki, M. F.; Greenlee, W. J.; McKittrick, B. A.; Parker, E. M.; Stamford, A. W. Structure based design of iminohydantoin BACE1 inhibitors: Identification of an orally available, centrally active BACE1 inhibitor. *Bioorg. Med. Chem. Lett*. **2012**, *22*, 2444–2449.
18. Stamford, A. W.; Scott, J. D.; Li, S. W.; Babu, S.; Tadesse, D.; Hunter, R.; Wu, Y.; Misiaszek, J.; Cumming, J. N.; Gilbert, E. J.; Huang, C.; McKittrick, B. A.; Hong, L.; Guo,T.; Zhu, Z.; Strickland, C.; Orth, P.; Voigt, J. H.; Kennedy, M. E.; Chen, X.; Kuvelkar, R.; Hodgson, R.; Hyde, L. A.; Cox, K.; Favreau, L.; Parker, E. M.; Greenlee, W. J. Discovery of an orally available, brain penetrant BACE1 inhibitor that affords robust CNS Aβ reduction. *ACS Med. Chem. Lett*. **2012**, *3*, 897-902.
19. (a) Wyss, D. F.; Cumming, J. N.; Strickland, C. O.; Stamford, A. W. BACE Inhibitors. In Fragment-based Drug Discovery: Lessons and Outlook; Erlanson D. A., Jahnke, W., Eds.; Wiley: New Jersey, 2016; Vol. 67, pp 329-353. (b) Stamford, A.; Strickland, C. Inhibitors of

BACE for treating Alzheimer's disease: a fragment-based drug discovery story. *Curr. Opin. Chem. Biol*. **2013**, *17*, 320-328.

20. (a) Hunt, K. W.; Cook, A. W.; Watts, R. J.; Clark, C. T.; Vigers, G.; Smith, D.; Metcalf, A. T.; Gunawardana, I. W.; Burkard, M.; Cox, A. A.; Geck Do, M. K.; Dutcher, D.; Thomas, A. A.; Rana, S.; Kallan, N. C.; DeLisle, R. K.; Rizzi, J. P.; Regal, K.; Sammond, D.; Groneberg, R.; Siu, M.; Purkey, H.; Lyssikatos, J. P.; Marlow, A.; Liu, X.; Tang, T. P. Spirocyclic β-site amyloid precursor protein cleaving enzyme 1 (BACE1) inhibitors: From hit to lowering of cerebrospinal fluid (CSF) amyloid β in a higher species. *J. Med. Chem*. **2013**, *65*, 3379–3403. (b) Malamas, M. S.; Erdei, J.; Gunawan, I.; Turner, J.; Hu, Y.; Wagner, E.; Fan, K.; Chopra, R.; Olland, A.; Bard, J.; Jacobsen, S.; Magolda, R. L.; Pangalos, M.; Robichaud, A. J. Design and synthesis of 5,5'-disubstituted aminohydantoins as potent and selective human β-secretase (BACE1) inhibitors. *J. Med. Chem*. **2010**, 53, 1146–1158. (c) Malamas, M. S.; Erdei, J.; Gunawan, I.; Barnes, K.; Johnson, M.; Hui, Y.; Turner, J.; Hu, Y.; Wagner, E.; Fan, K.; Olland, A.; Bard, J.; Robichaud. A. J. Aminoimidazoles as potent and selective human β-secretase (BACE1) inhibitors. *J. Med. Chem*. **2009**, 52, 6314–6323. (d) Barrow, J. C.; Stauffer, S. R.; Rittle, K. E.; Ngo, P. L.; Yang, Z.; Selnick, H. G.; Graham, S. L.; Munshi, S.; McGaughey, G. B.; Holloway, M. K.; Simon, A. J.; Price, E. A.; Sankaranarayanan, S.; Colussi, D.; Tugusheva, K.; Lai, M-T.; Espeseth, A. S.; Xu, M.; Huang, Q.; Wolfe, A.; Pietrak, B.; Zuck, P.; Levorse, D. A.; Hazuda, D.; Vacca. J. P. Discovery and X-ray crystallographic analysis of a spiropiperidine iminohydantoin inhibitor of β-secretase. *J. Med. Chem.* **2008,** *51,* 6259–6262. (e) Cole, D, C.; Manas, E. S.; Stock, J. R.; Condon, J. S.; Jennings, L. D.; Aulabaugh, A.; Chopra, R.; Cowling, R.; Ellingboe, J. W.; Fan, K. Y.; Harrison, B. L.; Hu, Y.; Jacobsen, S.; Jin, G.; Lin, L.; Lovering, F. E.; Malamas, M. S.; Stahl, M. L.; Strand, J.; Sukhdeo, M. N.; Svenson, K.; Turner, M. J.;

Wagner, E.; Wu, J.; Zhou, P.; Bard, J. Acylguanidines as small-molecule β-secretase inhibitors. *J. Med. Chem.* **2006**, *49,* 6158–6161. (f) Baxter, E. W.; Conway, K. A.; Kennis, L.; Bischoff, F.; Mercken, M. H.; De Winter, H. L.; Reynolds, C. H.; Tounge, B. A.; Luo, C.; Scott, M. K.; Huang, Y.; Braeken, M.; Pieters, S. M. A.; Berthelot, D. J. C.; Masure, S.; Bruinzeel, W. D.; Jordan, A. D.; Parker, M. H.; Boyd, R. E.; Qu, J.; Alexander, R. S.; Brenneman, D. E.; Reitz, A. B. 2-Amino-3,4 dihydroquinazolines as inhibitors of BACE-1 (β-Site APP cleaving enzyme): Use of structure based design to convert a micromolar hit into a nanomolar lead. *J. Med. Chem.* **2007,** *50,* 4162–4264. (g) Murray, C. W.; Callaghan, O.; Chessari, G.; Cleasby, A.; Congreve, M.; Frederickson, M.; Hartshorn, M. J.; McMenamin, R.; Patel, S.; Wallis, N. Application of fragment screening by X-ray crystallography to β-secretase. *J. Med. Chem.* **2007,** *50,* 1116–1123. (h) Congreve, M.; Aharony, D.; Albert, J.; Callaghan, O.; Campbell, J.; Carr, R. A. E.; Chessari, G.; Cowan, S.; Edwards, P. D.; Frederickson, M.; McMenamin, R.; Murray, C. W.; Patel, S.; Wallis, N. Application of fragment screening by X-ray crystallography to the discovery of aminopyridines as inhibitors of β-secretase. *J. Med. Chem.* **2007,** *50,* 1124–1132. (i) Geschwindner, S.; Olsson, L-L.; Albert, J. S.; Deinum, J.; Edwards, P. D.; Beer, T-D.; Folmer, R. H. A. Discovery of a novel warhead against β-secretase through fragment-based lead generation. *J. Med. Chem.* **2007,** *50,* 5903–5911. (j) Edwards, P. D.; Albert, J. S.; Sylvester, M.; Aharony, D.; Andisik, D.; Callaghan, O.; Campbell, J. B.; Carr, R. A.; Chessari, G.; Congreve, M.; Frederickson, M.;. Folmer, R. H. A.; Geschwindner, S.; Koether, G.; Kolmodin, K.; Krumrine, J.; Mauger, R. C.; Murray, C. W.; Olsson, L-L.; Patel, S.; Spear, N.; Tian. G. Application of fragment-based lead generation to the discovery of novel, cyclic amidine β-secretase inhibitors with nanomolar potency, cellular activity, and high ligand efficiency. *J. Med. Chem.* **2007,** *50,* 5912–5925. (k) Cheng, Y.; Judd, T. C.; Bartberger, M. D.; Brown, J.;

Chen, K.; Fremeau, Jr., R. T.; Hickman, D.; Hitchcock, S. A.; Jordan, B.; Li, V.; Lopez, P.; Louie, S. W.; Luo, Y.; Michelsen, K.; Nixey, T.; Powers, T. S.; Rattan, C.; Sickmier, E. A.; Jean, Jr., D. J. St.; Wahl, R. C.; Wen, P. H.; Wood. S. From fragment screening to *In Vivo* efficacy: optimization of a series of 2-aminoquinolines as potent inhibitors of beta-site amyloid precursor protein cleaving enzyme 1 (BACE1). *J. Med. Chem*. **2011**, 54, 5836–5857. (l) Ginman, T.; Viklund, J.; Malmstroem, J.; Blid, J.; Emond, R.; Forsblom, R.; Johansson, A.; Kers, A.; Lake, F.; Sehgelmeble, F.; Sterky, K. J.; Bergh, M.; Lindgren, A.; Johansson, P.; Jeppsson, F.; Faelting, J.; Gravenfors, Y.; Rahm, F. Core refinement toward permeable β secretase (BACE-1) inhibitors with low hERG activity. *J. Med. Chem*. **2012**, *55*, 4181–4205. (m) Tamura, Y.; Suzuki, S.; Tada, Y.; Yonezawa, S.; Fujikoshi, C.; Matsumoto, S.; Kooriyama, Y.; Ueno, T. Preparation of aminodihydrothiazine derivatives as BACE1 inhibitors. *PCT Int. Appl*. 2008133274, 2008. (n) Suzuki, Y.; Motoki, T.; Kaneko, T.; Takaishi, M.; Ishida, T.; Takeda, K.; Kita, Y.; Yamamoto,N.; Khan, A.; Dimopoulos, P. Preparation of condensed aminodihydrothiazine derivatives as inhibitors of β-site APP-cleaving enzyme 1 (BACE1). *PCT Int. Appl*. 2009091016, 2009.

21. Mandal, M.; Zhu, Z.; Cumming, J. N.; Liu, X.; Strickland, C.; Mazzola, R. D.; Caldwell, J. P.; Leach, P.; Grzelak, M.; Hyde, L.; Zhang, Q.; Terracina, G.; Zhang, L.; Chen, X.; Kuvelkar, R.; Kennedy, M. E.; Favreau, L.; Cox, K.; Orth, P.; Buevich, A.; Voigt, J.; Wang, H.; Kazakevich, I.; McKittrick, B. A.; Greenlee, W.; Parker, E. M.; Stamford, A. W. Design and validation of bicyclic iminopyrimidinones as beta amyloid cleaving enzyme-1 (BACE1) inhibitors: conformational constraint to favor a bioactive conformation. *J. Med. Chem*. **2012**, *55*, 9331–9345.

22. (a) May, P. C.; Dean, R. A.; Lowe, S. L.; Martenyi, F.; Sheehan, S. M.; Boggs, L. N.; Monk, S. A.; Mathes, B. M.; Mergott, D. J.; Watson, B. M.; Stout, S. L.; Timm, D. E.; Smith LaBell, E.; Gonzales, C. R.; Nakano, M.;. Jhee, S. S.; Yen, M.; Ereshefsky, L.; Lindstrom, T. D.; Calligaro, D. O.; Cocke, P. J.; Greg Hall, D.; Friedrich, S.; Citron, M.; Audia. J. E. Robust central reduction of amyloid-β in humans with an orally available, non-peptidic β-secretase inhibitor. *J. Neurosci*. **2011**, *31*, 16507–16516. (b) Jeppsson, F.; Eketjäell, S.; Janson, J.; Karlströem, S.; Gustavsson, S.; Olsson, L-L.; Radesäeter, A-C.; Ploeger, B.; Cebers, G.; Kolmodin, K.; Swahn, B-M.; von Berg, S.; Bueters, T.; Fäelting, J. Discovery of AZD3839, a potent and selective BACE1 inhibitor clinical candidate for the treatment of alzheimer disease. *J. Biol. Chem.* **2012**, *287*, 41245–41257. (c) May, P. C.; Willis, B,A.; Lowe, S.L; Dean, R.A.; Monk, S. A.; Cocke, P.J.; Audia, J.E.; Boggs, L. N.; Borders, A.R.; Brier, R.A.; Calligaro, D. O.; Day, T.A.; Ereshefsky, L.; Erickson, J. A.; Gevorkyan, H.; Gonzales, CR.; James, D.E.; Jhee, S.S.; Komjathy, S. F.; Li, L.; Lindstrom, T. D.; Mathes, B. M.; Marténvi, F.; Sheehan, S.M.; Stout, S. L.; Timm, D. E.; Vaught, G. M.; Watson, B. M.; Winneroski, L. L.; Yang, Z.; Mergott, D. J. The potent BACE1 inhibitor LY2886721 elicits robust central Aβ pharmacodynamic responses in mice, dogs, and humans. *J. Neurosci.* **2015**, *35*, 1199-1210. (d) Neumann, U.; Rueeger, H.; Machauer, R.; Veenstra, S. J.; Lueoend, R. M.; Tintelnot-Blomley, M.; Laue G.; Beltz, K.; Vogg, B.; Schmid, P.; Frieauff, W.; Shimshek, D. R.; Staufenbiel, M.; Jacobson, L. H. A novel BACE inhibitor NB-360 shows a superior pharmacological profile and robust reduction of amyloid-β and neuroinflammation in APP transgenic mice. *Mol. Neurodegener*. **2015**, *10*, 1-15. (e) Rombouts, F. J.; Tresadern, G.; Delgado, O.; Martínez-Lamenca, C.; Van Gool, M.; García-Molina, A.; Alonso de Diego S. A.; Oehlrich, D.; Prokopcova, H.; Alonso, J. M.; Austin, N.; Borghys, H.; Van Brandt, S.; Surkyn, M.; De Cleyn, M.; Vos, A.; Alexander, R.; Macdonald, G.; Moechars,

D.; Gijsen, H.; Trabanco. A. A. 1,4-Oxazine β-secretase 1 (BACE1) inhibitors: from hit generation to orally bioavailable brain penetrant leads. *J. Med. Chem*. **2015**, *58*, 8216-8235. (f) Cheng, Y.; Brown, J.; Judd, T. C.; Lopez, P.; Qian, W.; Powers, T. S.; Chen, J. J.; Bartberger, M. D.; Chen, K.; Dunn II, R. T.; Epstein, O.; Fremeau, R. T Jr.; Harried, S.; Hickman, D.; Hitchcock, S. A.; Luo, Y.; Minatti, A. E.; Patel, V. F.; Vargas, H. M.; Wahl, R. C.; Weiss, M. M.; Wen, P. H.; White, R. D.; Whittington, D. A.; Zheng, X. M.; Wood, S. An orally available BACE1 inhibitor that affords robust CNS Aβ reduction without cardiovascular liabilities. *ACS Med. Chem. Lett.* **2014**, *6*, 210-215. (g) Butler, C. R.; Brodney, M. A.; Beck, E. M.; Barreiro, G.; Nolan, C. E.; Pan, F.; Vajdos, F.; Parris, K.; Varghese, A. H.; Helal, C. J.; Lira, R.; Doran, S. D.; Riddell, D. R.; Buzon, L. M.; Dutra, J. K.; Martinez-Alsina, L. A.; Ogilvie, K.; Murray, J. C.; Young, J. M.; Atchison, K.; Robshaw, A.; Gonzales, C.; Wang, J.; Zhang, Y.; O'Neill, B. T. Discovery of a series of efficient, centrally efficacious BACE1 inhibitors through structure-based drug design. *J. Med. Chem*. **2015**, *58*, 2678−2702.

23. (a) Swahn, B-M.; Kolmodin, K.; Karlströem, S.; von Berg, S.; Söederman, P.; Holenz, J.; Berg, S.; Lindströem, J.; Sundströem, M.; Turek, D.; Kihlströem, J.; Slivo, C.; Andersson, L.; Pyring, D.; Rotticci, D.; Öehberg, L.; Kers, A.; Bogar, K.; Bergh, M.; Olsson, L-L.; Janson, J.; Eketjäell, S.; Georgievska, B.; Jeppsson, F.; Fäelting, J. Design and synthesis of β-site amyloid precursor protein cleaving enzyme (BACE1) inhibitors with in vivo brain reduction of β-amyloid peptides. *J. Med. Chem*, **2012**, *55*, 9346-9361. (b) Hilpert, H.; Guba, W.; Woltering, T. J.; Wostl, W.; Pinard, E.; Mauser, H.; Mayweg, A. V. Rogers-Evans, M.; Humm, R.; Krummenacher, D.; Muser, T.; Schnider, C.; Jacobsen, H.; Ozmen, L.; Bergadano, A.; Banner, D. W. Hochstrasser, R.; Kuglstatter, A.; David-Pierson, P.; Fischer, H.; Polara, A.; Narquizian, R. β-Secretase

(BACE1) Inhibitors with high in vivo efficacy suitable for clinical evaluation in Alzheimer's disease. *J. Med. Chem*. **2013**, *56*, 3980-3995.

24. Wilcken, R.; Zimmermann, M. O.; Lange, A.; Joerger, A. C.; Boeckler, F. M. Principles and applications of halogen bonding in medicinal chemistry and chemical biology. *J. Med. Chem*. **2013**, *56*, 1363-1388.
25. Rochin, L.; Hurbain, I.; Serneels, L.; Fort, C.; Watt, B.; Leblanc, P.; Marks,M. S.; De Strooper, B.; Raposo, G.; van Niel, G. BACE2 processes PMEL to form the melanosome amyloid matrix in pigment cells. *Proc. Natl. Acad. Sci. USA*. **2013**, *26*, 10658-10663.
26. Esterházy, D.; Stützer, I.; Wang, H.; Rechsteiner, M. P.; Beauchamp, J.; Döbeli, H.; Hilpert, H.; Matile, H.; Prummer, M.; Schmidt, A.; Lieske, N.; Boehm, B.; Marselli, L.; Bosco, D.; Kerr-Conte, J.; Aebersold, R.; Spinas, G. A.; Moch, H.; Migliorini, C.; Stoffel, M. BACE2 is a β cell-enriched protease that regulates pancreatic β cell function and mass. *Cell Metab*. **2011**, *14*, 365-377.
27. He, H.; Lyons, K. A.; Shen, X.; Yao, Z.; Bleasby, K.; Chan, G.; Hafey, M.; Li, X.; Xu, S.; Salituro, G. M.; Cohen, L. H.; Tang, W. Utility of unbound plasma drug levels and P glycoprotein transport data in prediction of central nervous system exposure. *Xenobiotica* **2009**, *39*, 687–693.
28. (a) Lu,Y.; Riddell, D.; Hajos-Korcsok, E.; Bales, K.; Wood, K. M.; Nolan, C. E.; Robshaw, A. E.; Zhang, L.; Leung, L.; Becker, S.L, Tseng, E.; Barricklow, J.; Miller, E. H.; Osgood, S.; O'Neill, B.T.; Brodney, M. A.; Johnson, D. S, Pettersson, M. Cerebrospinal fluid amyloid-β (Aβ) as an effect biomarker for brain Aβ lowering verified by quantitative preclinical analyses**.** *J. Pharmacol. Exp. Ther*. **2012**, *342*, 366-375. (b) Janson, J.; Eketjäll, S.; Tunblad, K.; Jeppsson, F.; Von Berg, S.; Niva, C.; Radesäter, A.-C.; Fälting, J.; Visser, S. A. G. Population PKPD

modeling of BACE1 inhibitor-induced reduction in Aβ levels in vivo and correlation to in vitro potency in primary cortical neurons from mouse and guinea pig. *Pharm. Res*. **2014**, *31*, 670–683. (c) Tai, L. M.; Jacobsen, H.; Ozmen, L.; Flohr, A.; Jakob-Roetne, R.; Caruso, A.; Grimm, H. P. The dynamics of Aβ distribution after γ-secretase inhibitor treatment, as determined by experimental and modelling approaches in a wild type rat. *J. Pharmacokinet. Pharmacodyn*. **2012**, *39*, 227-237. (d) Van Maanen, E.; Van Steeg, T.; Michener, M. S.; Savage, M. J.; Kennedy, M. E.; Kleijn, H. J.; Stone, J.; Danhof, M. Systems pharmacology analysis of the amyloid cascade enables the identification of an Aβ_{42} oligomer pool. *J. Pharmacol. Exp. Ther*. [Online early access]. DOI: 10.1124/jpet.115.230565. Published Online: January 29, 2016.

Table of Contents graphic

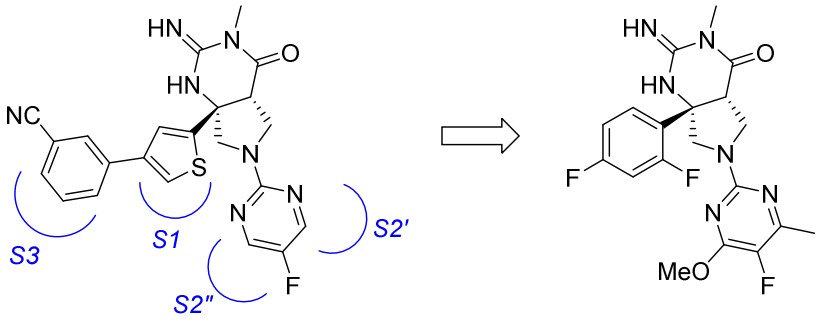

6 **9**